Mon. Not. R. Astron. Soc. **283,** 174–192 (1996)

Starburst galaxy contributions to extragalactic source counts

Chris Pearson and Michael Rowan-Robinson

Blackett Laboratory, Imperial College, Prince Consort Road, London SW7 2BZ

Accepted 1996 June 27. Received 1996 May 10; in original form 1994 November 11

ABSTRACT

Using detailed models of galaxy spectra, luminosity functions defined at 60 μm and pure luminosity evolution, the number–flux relation for extragalactic sources is constructed for wavelengths ranging from the submillimetre, through the infrared, to the *K*, *I* and *B* photometric bands. Such accurate source counts are vital for the preparation of possible survey strategies for the next generation of ground-based instruments and space-borne observatories such as SCUBA, *ISO* and *FIRST*.

The model consists of non-evolving spiral and elliptical components mixed with an evolving population of starburst galaxies, active galactic nuclei and a hyperluminous galaxy component. Pure luminosity evolution of the form $L(z)=L(0)(1+z)^{3.1}$ is used for all the evolving components. We show that, with this form of universal evolution, an excellent fit is found for both the source counts at 60 μm and the faint ($S<1$ mJy) radio counts at 1.4 GHz where the starburst galaxies are dominant. A new calculation of the infrared (IR) background comes interestingly close to the most recent *COBE* limits at 500 μm.

By extending our models to the near-IR we find that starburst galaxies only contribute to the *K* and *I* bands at the faintest magnitudes and that an open universe provides a better fit than closed world models, although this conclusion is highly dependent on the assumed form of the evolution.

In order to build a more complete picture of the extragalactic populations at various wavelengths, we directly connect the 60-μm and optical luminosity functions for spiral galaxies. For normal spiral galaxies emitting in the IR via IR 'cirrus' (re-radiation of starlight by interstellar dust), we confirm earlier findings that $\langle L_{IR}/L_B\rangle\approx 0.3$, supporting the idea that spiral galaxies are on average optically thin to dust. For starburst galaxies we constrain the escape fraction of optical light to 5–10 per cent, and suggest that a strongly evolving starburst component could explain the faint-blue galaxy excess and the increasing number of emission-line objects found in redshift surveys to $B\approx 22$–24, depending on the world model.

Key words: methods: statistical – galaxies: evolution – galaxies: starburst.

1 INTRODUCTION

In the wake of *IRAS*, great emphasis has been placed on observations in the infrared at wavelengths that were previously inaccessible from the ground. As well as increasing the understanding of areas such as interstellar medium, stellar and solar system studies, *IRAS* has had a profound impact on modern cosmology (for a review see Soifer, Houck & Neugebauer 1987). In particular, the *IRAS* all-sky survey has revealed an infrared sky dominated by dust emission and prolific in star formation, and has opened up an entirely new wavelength range to a host of cosmological queries and tests, previously confined mainly to optical wavelengths (e.g. Rowan-Robinson 1991). Of paramount importance is the study of the evolution of the various types of galaxies that make up the infrared population. The cosmological number–flux relation is ideal for such a study of evolution *IRAS* studies have provided all the necessary tools [*K*-corrections and luminosity functions (Saunders et al. 1990)] for these calculations.

This paper introduces a new model for the infrared (IR) source counts of extragalactic populations, using the information provided by the wealth of *IRAS* studies to predict the number of extragalactic sources at wavelengths ranging from the radio, to the submillimetre, where many high-redshift objects may be found, through the far-infrared (FIR) to the near-infrared (NIF) *K* and *I* bands.

Earlier calculations of this type have been made by Franceschini et al. (1991) and Blain & Longair (1993), who provided predictions for source counts over a wide range of wavelengths from the submillimetre to the *K* band using mean spectra derived from *IRAS* data and simple black body models, respectively, to model the spectra of galaxies in the FIR. In this paper we incorporate a more careful treatment of galaxy spectral energy distributions (SEDs) constructed using the radiative transfer models of Rowan-Robinson & Efstathiou (1993) and the IR luminosity function of Saunders et al. (1990) to make detailed predictions from the submillimetre to NIR wavelengths.

Furthermore, we seek to connect the emission from galaxies at different wavelengths in order to build a more complete picture of how contributions to the source counts from the different extragalactic populations vary with wavelength. In particular, we examine the possible impact of a strongly evolving IR starburst galaxy component on the counts at shorter (NIR and optical) wavelengths. Recently, in the *B* band it has been popular to postulate galaxies at moderate redshifts that are undergoing a strong starburst episode (e.g. Treyer & Silk 1993) as being responsible for the observed faint blue galaxy excess of Tyson (1988) at faint *B* magnitudes (at least to $B \approx 24$). It is possible that the *IRAS* 60-μm starburst population could provide an explanation for at least some of the observed excess (but see Tresse et al. 1996).

The sections are set out as follows. In Section 2 a new model for predicting the IR source counts is introduced, including the choice and treatment of galaxy SEDs, cosmological model and evolution. Section 3 deals with the model predictions in the FIR, submillimetre and radio, and includes a new model for the IR background radiation. Section 4 investigates the contribution of the IR starburst galaxy population to the NIR and optical source counts. In Section 5 the models are used to identify the wavelengths of interest and to optimize any possible observing strategies for the next generation of ground-based instruments and space-borne observatories dedicated to studies at submillimetre and IR wavelengths. The conclusions are given in Section 6.

Throughout this paper, unless otherwise specified, an Einstein–de Sitter universe ($\Omega = 1$, $\Lambda = 0$) is assumed with $H_0 = 50$ km s^{-1} Mpc^{-1}.

2 A NEW MODEL FOR SOURCE COUNTS IN THE IR

2.1 Galaxies in the IR

The IR region of the electromagnetic spectrum is where a large fraction of a galaxy's energy is radiated, accounting in some cases for as much as 99 per cent of a galaxy's total emission. Furthermore, unlike the optical and UV regions, emission in the IR suffers minimal extinction by dust and gas between the observer and the emitting source (Mathis 1990).

To model the counts in the IR we propose a multicomponent model comprising the major contributors in the FIR. Using a sample of 227 galaxies from the *IRAS* Point Source Catalogue with IR fluxes measured in all four *IRAS* bands (12, 25, 60 and 100 μm), Rowan-Robinson & Crawford (1989) constructed 12–25–60 and 25–60–100 μm colour–colour diagrams. They found that individual, identifiable galaxy types inhabited distinct, separate and well-defined areas in the colour–colour diagrams. Hence the individual components responsible for the overall emission from the galaxies could be identified and modelled independently. Each component is responsible for the majority of the emisson over specific wavelength ranges.

A cool cirrus component, which is simply dust heated by the interstellar radiation field (Low et al. 1984), equivalent to the emission observed from the clouds (hence the name cirrus) of neutral interstellar gas seen in the Milky Way, is representative of the emission from the majority of normal, spiral (disc) galaxies. The cirrus emission peaks at 100 μm, although it has also been detected at 60, 25 and 12 μm (Gautier & Beichman 1985). A warmer starburst component dominates emission at 50–100 μm, peaking at about 60 μm [Weedman et al. (1981) define a starburst galaxy as any galaxy undergoing an active phase of intense star formation usually in the central region of the galaxy]. The starburst spectrum is distinguishable by a huge hump of thermal dust emission in the FIR and is correlated with the optical emission, since the dust emission is reprocessed starlight from a population of young, hot O stars (Rowan-Robinson, Helou & Walker 1987). Such stars will be short-lived (10^6–10^7 years) and will end their lives as supernovae. The subsequent radio emission from synchrotron radiation in supernova remnants is tightly correlated with the IR emission (e.g. Helou, Soifer & Rowan-Robinson 1985; Condon 1992). Finally, a hot Seyfert component, peaking at 25 μm, that for radio-quiet active galactic nuclei from the FIR to the submillimetre (e.g. Edelson, Malkan & Reike 1987; Hughes et al. 1993; Vaceli et al. 1993) can be attributed to thermal emission from dust that is heated by the active galactic nucleus (AGN), a central engine at the heart of the galaxy, possibly a black hole (but see Terlevich & Melnick 1985 for alternative explanation for this emission). Although all AGN (excluding blazars) exhibit a minimum near 1 μm due to the dust evaporation by the central source, some type 1 Seyferts and radio-loud quasars [which would account for only 5 per cent of an optically selected sample of AGN (Condon et al. 1981)] may emit non-thermal radiation into the FIR.

The spectra of all these components have been modelled successfully using the interstellar dust-grain families and radiative transfer calculations of Rowan-Robinson (1980, 1992) and Rowan-Robinson & Efstathiou (1993), and are shown in Fig. 1 (see Savage & Mathis 1979; Hildebrand 1983; Draine & Lee 1984; Rowan-Robinson 1986; Mathis 1990 and Rowan-Robinson 1992, for a review of interstellar grain families and dust models).

In addition to the above three components we introduce a new component – the hyperluminous galaxy. The justification for this is the recent discovery of objects such as the $z = 2.286$ primeval emission-line galaxy F10214 + 4724, with a bolometric luminosity in excess of 3×10^{14} L$_\odot$ ($H_0 = 50$ km s^{-1} Mpc^{-1}, $\Omega = 1$, Rowan-Robinson et al. 1991), which may be a new class of IR galaxy. Although Graham & Liu (1996), Elston et al. (1994) and Matthews et al. (1994) have shown that F10214 exhibits arc-like morphology indicative of gravitational lensing by an early-type galaxy at $z=0.42$, the bolometric luminosity would only be reduced to $1.48–4\times10^{13}\,L_\odot$, still making it one of the most luminous galaxies in the Universe (Close et al. 1995; Trentham 1995). Lawrence et al. (1994) have shown that it is likely that F10214 is a composite object similar to NGC 1068 in exhibiting both quasar- (Lawrence et al. 1993; Rowan-Robinson et al. 1993a) and starburst-like components (Ebaz et al. 1992; Solomon, Downes & Radford 1992; Telesco 1993; Green & Rowan-Robinson 1996; Matthews et al. 1994). Norman & Scoville (1988) have proposed that many ultraluminous starburst galaxies may eventually evolve to AGN and Clements et al. (1996a) have shown that ≈35 per cent of a sample of 91 ultraluminous *IRAS* galaxies may harbour an AGN. The optical–NIR continuum can be fitted (unlike the quasar model) using the 9×10^8-year-old starburst model for high-redshift radio galaxies of Chambers & Charlot (1990).

In this paper we use the starburst model B of Rowan-Robinson et al. (1993a) to model the submillimetre to the mid-IR spectrum of F10214. Predicted number counts of such sources will help in choosing how to optimize the parameters for possible searches for these objects.

2.2 The cosmological model

Once the natures of the different populations of extragalactic sources have been established, their contributions to the total number of sources at different wavelengths can be investigated.

For any population, the number of sources observed per steradian at frequency ν_0 in the luminosity range L_l–L_u out to a limiting flux S is given by

$$N_{\nu_0}(S)=\int_{L_l}^{L_u} \mathrm{d}\log L \int_0^{z(L,S)} \phi(L,z)\,\mathrm{d}V, \qquad (1)$$

where

$$L=L(\nu_0), \qquad S=S(\nu_0), \qquad \phi(L,z)=\phi[L(z),0].$$

ϕ is defined as the differential luminosity function per decade in luminosity ($\phi=\mathrm{d}\Phi/\mathrm{d}\log L$ where Φ is the number density of galaxies with luminosity in the range L, $L+\mathrm{d}L$). The volume element (per steradian) $\mathrm{d}V=r^2R^3\,\mathrm{d}r$ is easily integrated for an Einstein–de Sitter universe to give the volume enclosd at redshift z:

$$V[z(L,S)]=\frac{1}{3}\left(\frac{2c}{H_0}\right)^3[1-(1+z)^{-1/2}]^3. \qquad (2)$$

The limiting redshift z depends upon the flux limit S_{ν_0} at which a galaxy of luminosity L will drop out of the sample, where S_{ν_0} is given by

$$S_{\nu_0}=\frac{L_{\nu_e}}{4\pi D_L^2}(1+z)=\frac{L_{\nu_0}}{4\pi D_L^2}\left(\frac{\nu_e L_{\nu_e}}{\nu_0 L_{\nu_0}}\right), \qquad (3)$$

where ν_e denotes the source rest frame and D_L is the luminosity distance given by

$$D_L=R_0 r(1+z)=(2c/H_0)[(1+z)-(1+z)^{1/2}]$$

(e.g. Narlikar 1993). The last factor in equation (3) is the K-correction.

To model the source counts, a three-component model (plus hyperluminous component) similar to that of Rowan-Robinson & Crawford (1989) is used which covers the full range of possible observed luminosities from $\log(L/L_\odot)=6$, typical of Local Group dwarf galaxies, to the most luminous objects in the Universe, $\log(L/L_\odot)=14$. The number densities of sources in the IR have been fitted by the luminosity function of Saunders et al. (1990), who defined individual luminosity functions for the different IR source populations described by

$$\phi(L)=\frac{\mathrm{d}\Phi}{d\log L}=C\left(\frac{L}{L^*}\right)^{1-\alpha}\exp\left[-\frac{1}{2\sigma^2}\log^2\left(1+\frac{L}{L^*}\right)\right]. \qquad (4)$$

This luminosity function is defined at 60 µm, and hence the above luminosity limits correspond to the 60-µm luminosity where $L_{60}=\nu_{60}L_\nu$. For normal spiral galaxies in the IR, the cirrus (cool-component) luminosity function is used over the range $\log(L_{60}/L_\odot)=6–11.5$ (see Table 1). Starburst galaxies are represented by the starburst (warm-component) luminosity function over the range $\log(L_{60}/L_\odot)=6–12.5$ (see Table 1). A high-luminosity component, $\log(L_{60}/L_\odot)=6–12.5–14.0$, using the warm-component luminosity function but a different SED, is used to represent the ultraluminous and hyperluminous (e.g. F10214) *IRAS* galaxies, under the assumption that starburst is the major mechanism behind such objects (Condon et al. 1991a).

For the AGN luminosity function, we use the information collected by Rush, Malkan & Spinoglio (1993) in their 12-µm galaxy sample – an all-sky 12-µm flux-limited sample

Table 1. Luminosity function parameters for the cases described in the text.

Luminosity Function	α	σ	$lg(L^*/L_\odot)$	$\phi^*(\mathrm{Mpc}^{-3})$	C ($ln10\,\phi^*$)
Saunders *et al.* (1990) Cirrus (line 24)	1.15	0.463	9.62	8.69×10^{-4}	2.0×10^{-3}
Saunders *et al.* (1990) Starburst (line 25)	1.27	0.626	9.99	1.41×10^{-4}	3.25×10^{-4}
Schecter (Loveday *et al.* 1992)	-0.97†	-	10.23	1.75×10^{-3}	4.03×10^{-3}

‡The change in sign of α is due to the definition of the luminosity functions.

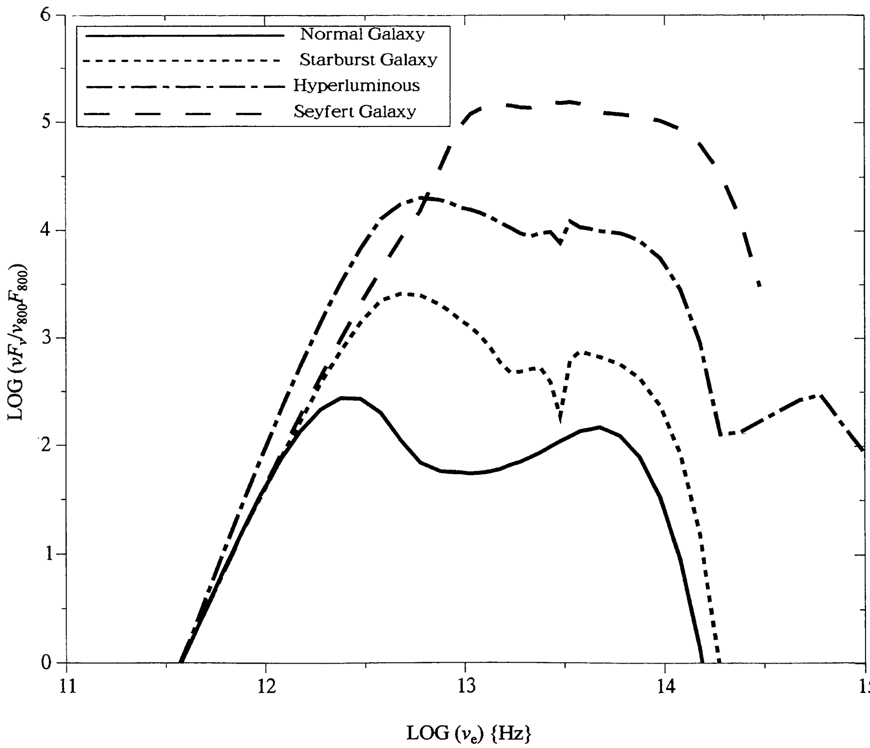

Figure 1. Model spectral energy distributions of cirrus, starburst, hyperluminous and Seyfert galaxy components in the IR.

of 893 galaxies from the *IRAS* Faint Source Catalogue (version 2), of which 117 were AGN (53 type 1 Seyfert and quasars, 63 type 2 Seyferts and two blazars). The 12-μm luminosity function was fitted by the 2 power-law parametrization of Lawrence et al. (1986) derived from a sample of 303 galaxies at 60 μm (although the numer of AGN detected in this survey was low). Rush et al. (1993) modelled their type 1 Seyfert/quasar/blazar and type 2 Seyfert components separately, and found that AGN started to dominate their counts at $L_{12} \sim 10^{10.8}\,L_\odot$ and that all galaxies above $L_{12} \sim 10^{11.2}\,L_\odot$ harboured an AGN. The space densities of the type 2 Seyfert and type 1 Seyfert galaxies were approximately equal.

Note that the E/S0 population is not represented since the *IRAS* satellite was not sensitive to these galaxies (Soifer et al. 1987), and hence counts at shorter wavelengths (i.e. in the NIR), where the emission from older Population II red stars is dominant (Telesco 1993), will provide a lower limit since only the spirals are represented. However, the strong evolution (see Section 2.3) invoked for the starburst galaxies back to high redshifts ($z = 5-10$) may perhaps be interpreted as the contribution from star formation in early elliptical galaxies.

Since the predictions for source counts are to be examined over a large range of wavelengths, no simple power law can be assumed for the *K*-correction. Instead, using the data from Section 2.1, the SEDs (i.e. the shape of the spectrum) are used to define the *K*-corrections that are required for any source (see Fig. 1). For the normal, quiescent galaxies, the cirrus model of Rowan-Robinson (1992) is used. The models of Rowan-Robinson & Efstathiou (1993) provide a good fit to the starburst component, and similar models (with a higher optical depth) have been used to model the hyperluminous *IRAS* galaxies (e.g. Rowan-Robinson et al. 1993a). For the AGN, *K*-corrections have been derived from models for the IR emission of quasars from Rowan-Robinson (1995), where the IR spectra of 24 PG quasars with *IRAS* detections were fitted using a two-component model consisting of emission from dust clouds in the narrow-line region for $\lambda = 3-30$ μm and a starburst-type component to contribute to the emission at $\lambda = 30-100$ μm.

The maximum redshift (i.e. redshift of formation) is chosen arbitrarily to be 10. Since quasars are known to exist out to redshifts of almost 5, however, it seems reasonable to assume that the formation of the host galaxy must have begun at even greater redshifts. In any case, since the volume in an Einstein–de Sitter universe does not increase significantly with redshift for $z \gg 1$, any extra volume at high redshifts will be negligible and will not drastically affect the resulting counts.

2.3 Cosmological evolution

It is generally accepted that some form of evolution is needed for all populations of active sources (e.g. QSOs, radio galaxies and starburst galaxies) in order to model extragalactic source counts successfully.

One of the most significant studies of quasar evolution was carried out by Boyle et al. (1987, 1988), who used a sample of over 400 UVX (ultraviolet excess) selected quasars in the optical to deduce that their source counts were best fitted with pure luminosity evolution of the form $L(z,=L(0)(1+z)^k$ (see equation 5), with $k = 3.1$. In this scenario, quasars are considered to be short-lived objects ($\sim 10^8$ yr), strongly evolving after forming at $z > 2$, the space density of quasars at redshifts of 2–5 remaining constant (although some density evolution may be needed to reconcile the counts with the faintest $M_B > -23$ quasars). A similar evolution rate, $k = 3.16$, was found by Padovani (1993) for the PG sample of quasars; however, studies by Miller et al. (1993) and Goldschmidt et al. (1992) using the Edinburgh UVX quasar survey suggest a lower rate of evolution. The evolution of quasars has also been studied at radio wavelengths (Dunlop & Peacock 1990) and in the X-ray region, where Maccacaro et al. (1991) and Della Ceca et al. (1992) have used the Einstein Observatory Extended Medium-Sensitivity Survey (EMSS) to collect a sample of over 400 quasars to deduce a lower evolutionary rate of $k = 2.56$, significantly lower than in the optical. Recent work using data from *ROSAT* suggests a value of $k = 2.8$ (Boyle et al. 1993). We adopt

$$L(z) = L(0)(1+z)^{3.1} \quad \text{for } z <,$$
$$L(z) = L(z=2) \quad \text{for } z > 2, \qquad (5)$$
$$\phi = 0 \quad \text{for } z > 10.$$

It is likely, given the amount of observed star formation, that a large component of the IR population has evolved to the present epoch. Possible scenarios are density evolution, where, due to merging/interactions, galaxies were more numerous in the past, or luminosity evolution, where, due to star formation, galaxies were more luminous in the past. Clements et al. (1996b) have shown that mergers/interactions drive the emission of 91 per cent of their sample of ultraluminous *IRAS* galaxies selected from the *IRAS* Faint Source Survey. Such evolution produces a steepening in the number counts. At 60 μm, Lonsdale et al. (1990) used the *IRAS* Faint Source Survey to demonstrate the steep slope of the faint 60-μm counts, concluding that the dominant population consisted of starburst galaxies which were strongly evolving. Saunders et al. (1990), Oliver et al. (1995) showed that both luminosity (with a rate of $k \approx 3$) and density evolution were consistent with the redshift distribution of the QDOT sample.

At radio frequencies (1.4 GHz), Benn et al. (1993) identified two important source groups. The bright (i.e. radio-loud) radio sources (giant ellipticals and quasars) and a fainter population consisting of spirals (starbursts and radio-quiet quasars). This faint population caused the upturn at low flux in the differential counts. Furthermore, it was found that this starburst population was indistinguishable from the faint 60-μm population. Thus, from 60 μm to radio wavelengths (for spirals, ultraluminous galaxies and radio-quiet quasars), it appears that we are just seeing starburst activity; i.e., there is no black hole power source involved (Sopp & Alexander 1991; Condon et al. 1991a; but see Lonsdale, Smith & Lonsdale 1995; Rigopoulou, Lawrence & Rowan-Robinson 1996). Rowan-Robinson et al. (1993b) have shown that the faint radio spiral population counts can be fitted by a model using pure luminosity evolution of a similar form to the optical quasar evolution rate (equation 5). The necessity for luminosity evolution of the bright radio source population is well established (e.g. Rowan-Robinson 1970, Condon 1984a, Dunlop & Peacock 1990).

In this paper, pure luminosity evolution of the form in equation (5) is adopted for the starburst, hyperluminous and Seyfert components.

3 SOURCE COUNTS IN THE SUBMILLIMETRE AND FIR

3. Model predictions

Using the model description in the previous section, source counts can be predicted throughout the submillimetre and FIR. At wavelengths other than 60 μm, where the luminosity function is defined, the luminosity range (L_1, L_u) must be shifted by a factor $\Delta = L(\nu)/L_{60}$. The luminosity function of the sources at the new frequency, ν is given by $\phi_\nu(L) = \phi_{60}(K_{60}\Delta)$.

From Fig. 1, it can be seen that the *K*-corrections, especially in the submillimetre, are expected to be very significant due to the steepness of the spectrum at thse wavelengths. To investigate this, the flux–redshift curves (the sensitivity that must be attained to include a source of luminosity L at redshift z in the sample) for a luminosity of $10^{11}\,L_\odot$ are plotted in Fig. 2 for the starburst component. The results are striking (see Franceschini et al. 1991; Blain & Longair 1993). At wavelengths longer than ≈ 100 μm, instead of the expected inverse-square fall-off with increasing redshift, the *S*–*z* curves in fact start to increase with redshift. What is happening is that, at wavelengths longwards of 100 μm, as the redshift increases, the dust-emission peak is shifted into the observation window. The effect of this is to produce a large 'second' volume that suddenly becomes accessible, making detection of galaxies at high redshift easier than those at lower redshift. Such an effect will have exciting implications for the next generation of instruments in the submillimetre such as the Sub-mm Common User Bolometric Array (SCUBA) and the *Far-IR Space Telescope* (*FIRST*).

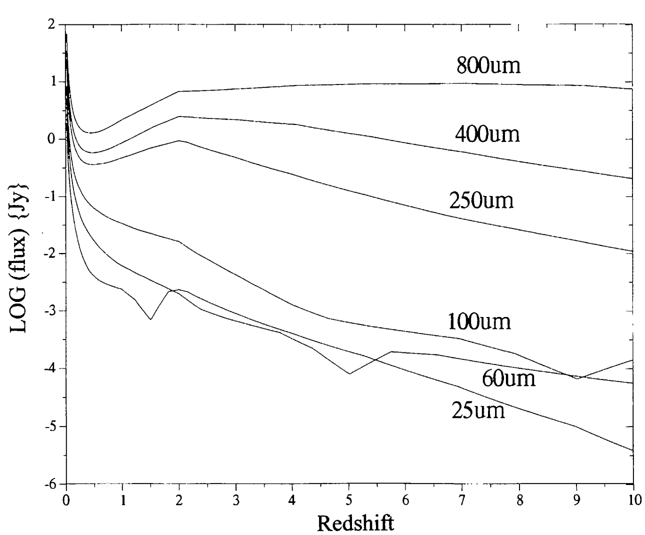

Figure 2. Flux–redshift relation for wavelengths (in μm) from the submillimetre to mid-IR for the model starburst galaxy component using a luminosity of $10^{11}\,L_\odot$ and highlighting the inversion due to the strong *K*-corrections. The magnitude of the inversion increases with wavelength.

The joint effect of the strong K-correction and luminosity evolution is to produce counts with large excesses over Euclidean predictions.The integral counts at a selection of wavelengths from the FIR to submillimetre are plotted in Fig. 3 and agree well with the predictions of Franceschini et al. (1991). Emission in the mid-IR (5–30 μm) is provided by hot dust (> 100 K) heated by young massive stars, or, in the case of AGN, by the central compact source. The FIR (30–300 μm) is dominated by the re-radiation of stellar emission by cooler (30–50 K) grains and has a characteristic thermal shape. Finally, the submillimetre emission (300 μm to 1 mm) from galaxies can be explained by the emission from ~20–30 K dust grains. The results correlate well with the increasing prominence of the S–z inversion with wavelength. The excess humps, prominent especially in the submillimetre, are due to the evolving starburst component, and the 'kinks' seen at the longer wavelengths mark a change in the volume being sampled at that flux (i.e. when the flux corresponds to the minimum of the S–z curve for example). Blain & Longair (1993), who used a single dust temperature to model their source SEDs, found that their predicted counts depend heavily on the assumed dust temperature. Their calculations, using evolving (isothermal dust temperature) models with grain temperatures of 30 and 60 K, predicted 175 and 0.5 sources per square degree respectively at 0.1 Jy and 450 μm. In this paper we predict ≈4 sources per square degree, closer to their higher-temperature model. Note that, unlike the alternative models of, for example, Franceschini et al. (1994), we have not explicitly included a dusty elliptical component in the IR models, but, because we incorporate an evolving starburst component to high redshift, some of this contribution may be considered as being from star formation in early high-redshift elliptical galaxies.

The differential counts normalized to the Euclidean value of $dN/dS \propto S^{-5/2}$ are plotted in Fig. 4 and show a spectacularly large excess hump at fluxes from 10^{-2} to 10^{-3} Jy (due to the inversion discussed previously), only flattening to Euclidean values at brighter fluxes. Starburst galaxies are the dominant component for all wavelengths greater than ≈50 μm and are found at consistently higher redshifts than the cirrus galaxies. Source counts of the hyperluminous component are always at least an order of magnitude below that of both the cirrus and the starburst galaxies. The number of AGN is quite low at fluxes of 0.01 Jy and brighter, but begins to make a more significant contribution to the total counts at fainter flux levels. Type 1 and type 2 Seyferts are present in approximately equal proportions. The majority of the AGN in the FIR and in the submillimetre are expected to be at high redshift.

3.2 Source counts at 60 μm

Perhaps the most intensively studied wavelength in the FIR is at 60 μm, where the predictions of the model can be compared with the data collected by the *IRAS* satellite. The 60-μm counts are plotted in different form, per steradian, normalized to Euclidean space in Fig. 5. The fit to the observed values compiled by Oliver et al. (1992) is extremely good, with the starburst galaxies dominating (especially at fainter fluxes), as is expected at 60 μm since the dust emission for starburst galaxies peaks here. Less than 0.1 hyperluminous objects are expected per square degree at 0.1 Jy. The number of AGN expected is negligible until fainter flux levels ($S \approx 10^{-2}$–10^{-3} Jy) are approached. Also shown in Fig. 5 is the effect on the source counts of the adoption of a lower rate of luminosity evolution for the starburst galaxy component. Using the lower rate of $L(z) = L(0)(1+z)^2$, which is within the range currently permitted by observation (Oliver et al. 1995), we find that, although the fit to the counts at the brightest fluxes is preserved (where the starburst counts are augmented by the contribution from the cirrus galaxies), the fit below the subjansky level falls short of the observed values.

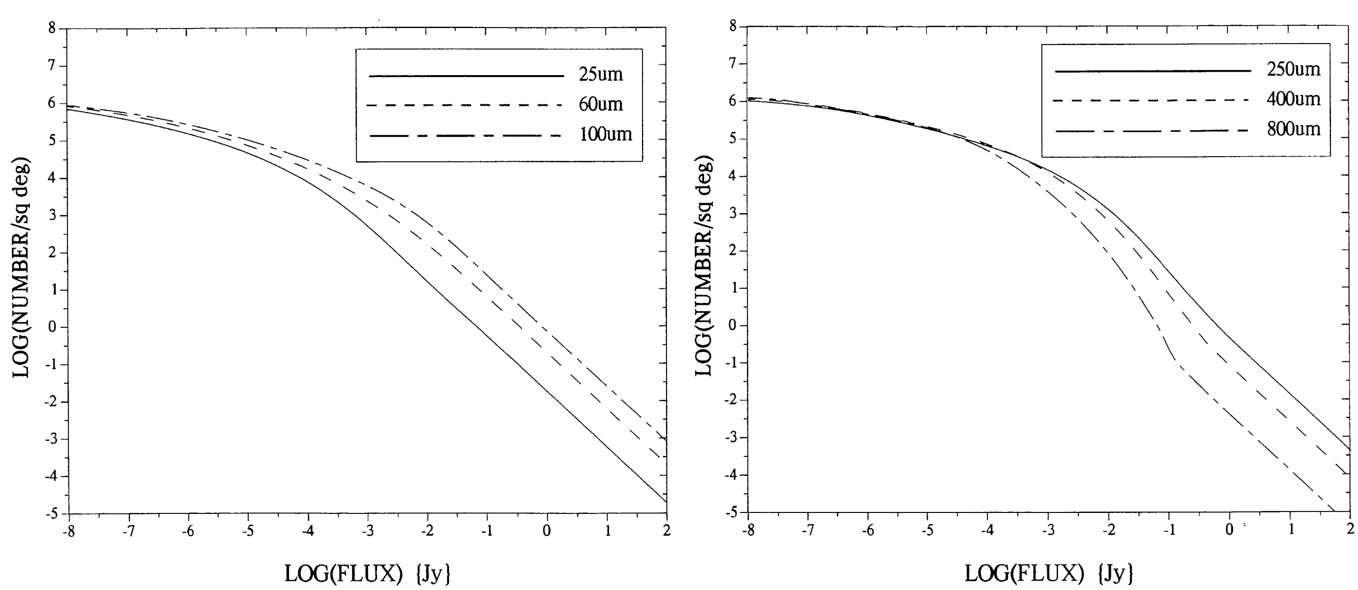

Figure 3. Predicted integral counts for IR wavelengths for the four-component model. The hump seen with increasing prominence with wavelength is mainly due to the K-corrections and evolution of the starburst component.

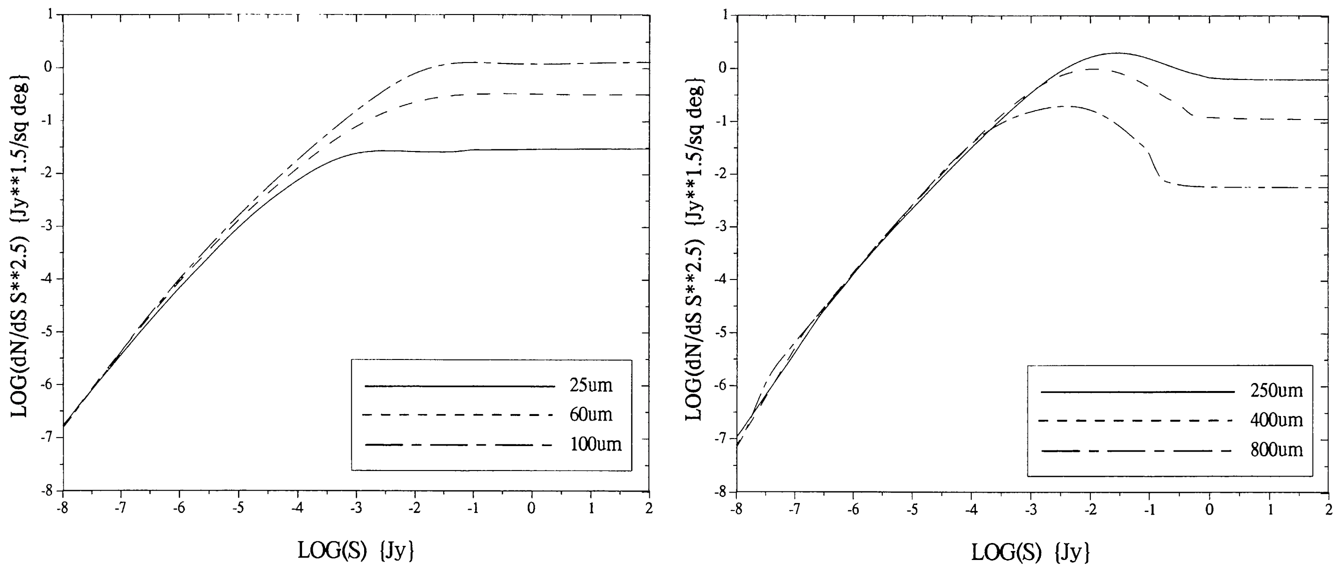

Figure 4. Predicted normalized differential counts for IR wavelengths for the four-component model. In the submillimetre, the effect of the K-correction and evolution produce counts well in excess of Euclidean.

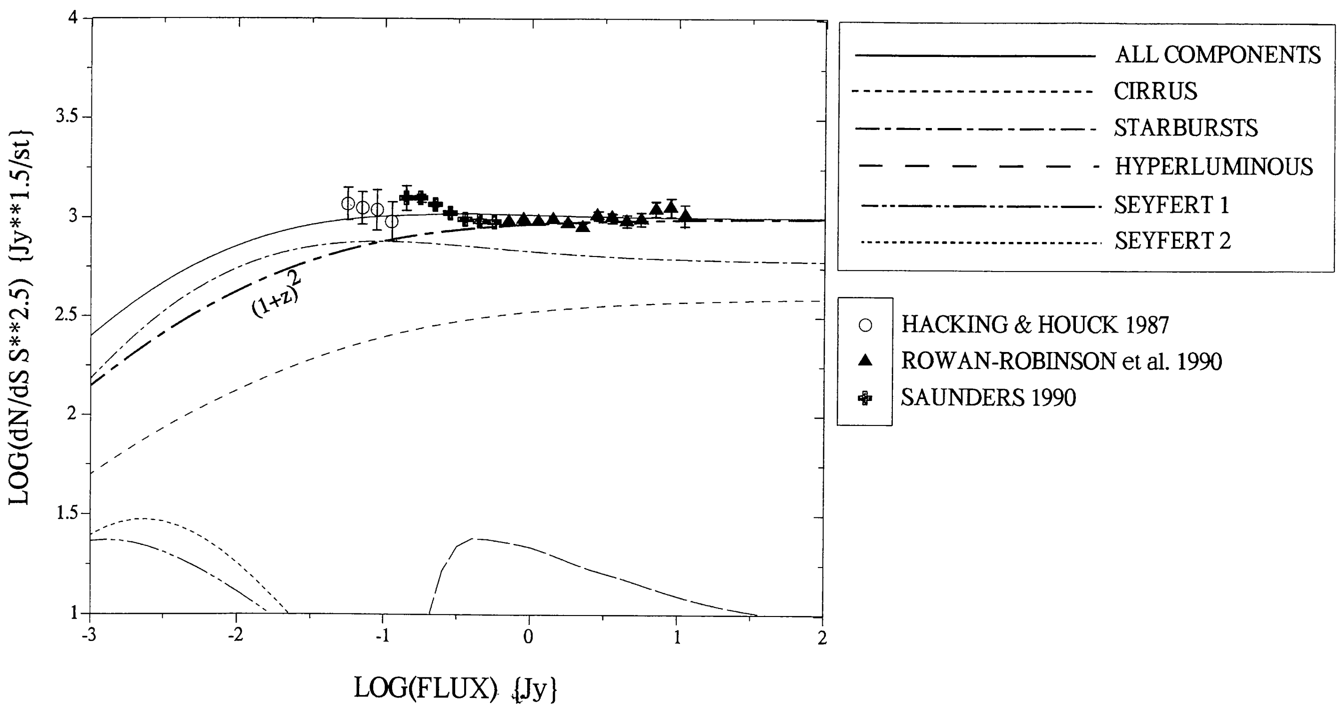

Figure 5. Fit of the four-component (cirrus, starburst, Seyfert and hyperluminous) model to the observed counts at 60 μm compiled by Oliver et al. (1992). Also shown (in bold) is the effect on the counts of incorporating a lower evolution rate of $(1+z)^2$ for the starburst component.

There is some question over the effect of large-scale structure on the 60-μm source counts. Although source counts in the FIR are less susceptible to large-scale structure than in the optical (a factor of 2 lower in the contrast between supercluster and void), because of the greater mean distance of surveys and the fact that IR surveys preferentially detect spirals, which are more commonly found in the field rather than ellipticals which are more common in clusters, there still exists a count anisotropy between the northern and southern sky counts. This discrepancy can be modelled as either a supercluster in the north (overdensity) or void (underdensity) in the south. Lonsdale et al. (1990) used the *IRAS* Faint Source Survey (FSS, Moshir et al. 1989) to show that known structures are not responsible for the discrepancies between the north and south counts, that counts below $\log f_{60}=0.1$ cannot be due to a local supercluster and that some evolution is necessary whatever the discrepancies due to large-scale structure. Oliver et al.

(1995) have shown that by eliminating local large-scale structure by discarding galaxies with $z<0.02$ the evolution rate is still $k=3.3\pm0.8$.

In order to distinguish fully between large-scale structure and evolution, a sufficiently large volume of space needs to be sampled. Deeper observations, such as will be provided by the *Infra-red Space Observatory* (*ISO*), will go some way to providing such answers and will also fully constrain the evolutionary parameters.

3.3 Contributions to the IR background radiation

The IR background radiation due to diffuse emission and the superposition of unresolved sources is given by

$$I_{(\nu)}=\int_0^{\infty} S_\nu \, dN(S_\nu),$$

where the intensity in W m^{-2} sr^{-1} Hz^{-1} is found by integrating over all fluxes for all sources. In this case, however, because the integral counts in the models can be predicted to very faint fluxes, the background intensity can be found by summing over the integral counts:

$$I_{(\nu)}=\sum_S DS_\nu \, dN(S_\nu).$$

Fig. 6 shows the predicted background compared with the upper limits derived from *COBE*. Our results are in general agreement with those of Beichman & Helou (1991), Franceschini et al. (1991), Oliver, Rowan-Robinson & Saunders (1992) and Blain & Longair (1993), although models invoking density evolution tend to predict slightly higher values of the background radiation longwards of 100 μm than the models presented in this paper. As can be seen, the predictions are still well within the latest upper limits from DIRBE (Hauser 1996) but intriguingly close to the 500-μm *FIRAS* limit (Mather et al. 1994).

3.4 Faint radio source counts

Source counts carried out in the radio over the range 0.5–5 GHz (e.g. Condon 1984a) can be understood by dividing the contributions into two general morphological classes. At fluxes brighter than 1 mJy the majority of sources are ellipticals while at fainter fluxes the contribution to the source counts is associated with spiral galaxies.

Models for the source counts of the bright radio sources (the ellipticals) can only be reconciled with observation if some form of evolution is assumed. For example, Dunlop & Peacock (1990) have shown that by using pure luminosity evolution (of luminous sources) both the count and redshift data can be fitted.

Source counts at fainter flux levels show an upturn at a radio flux of ≈1 mJy (Condon 1984b; Windhorst 1984). This flattening of the differential counts was interpreted as being due to a new population of extragalactic sources which at 1 mJy comprised approximately one-third of the total counts (the remaining two-thirds consisting of the elliptical component). Spectroscopic evidence collected by Thuan & Condon (1987) and Benn et al. (1993) has shown

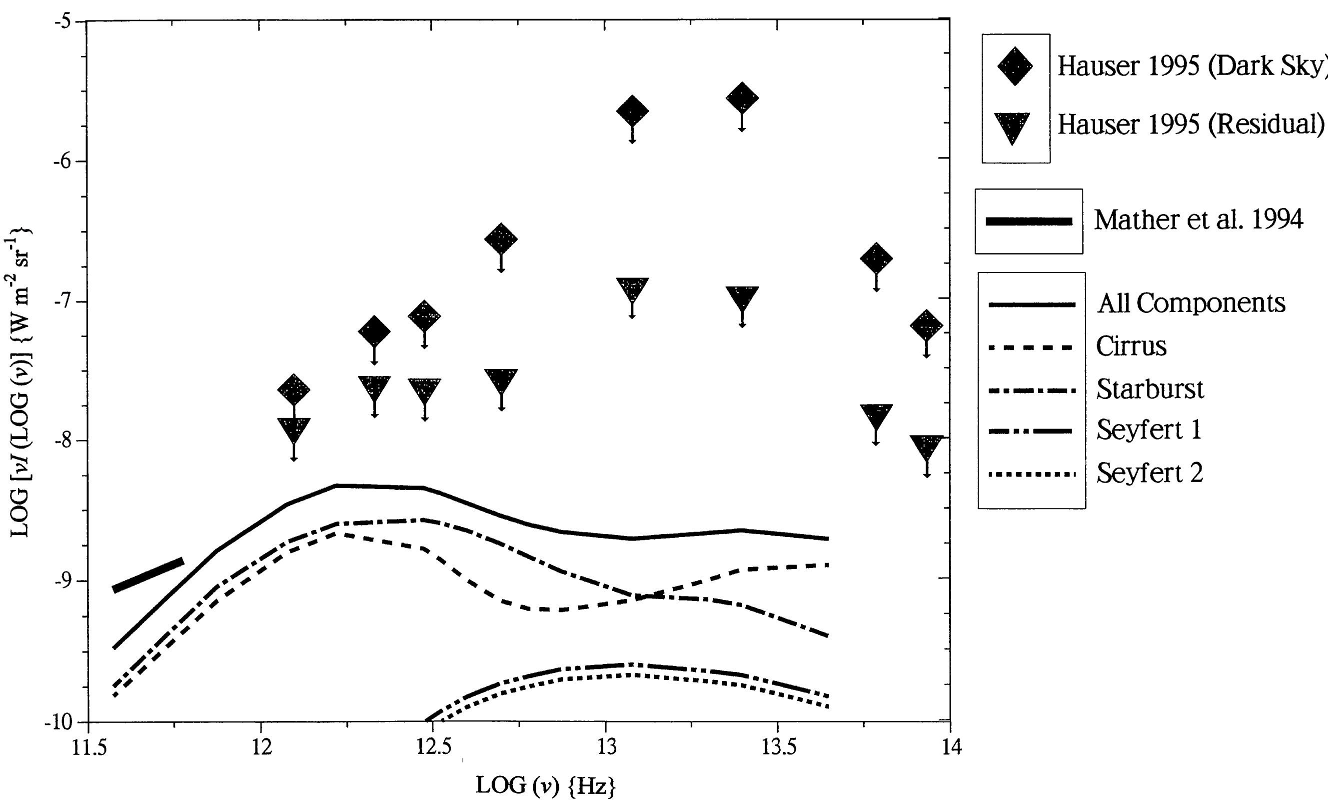

Figure 6. Model contributions to the FIR background radiation compared with the latest *COBE*.

that the submJy population comprises active star-forming galaxies with a median redshift of ≈ 0.25. Mitchell & Condon (1985), Thuan & Condon (1987), Danese et al. (1987), Francheschini et al. (1988) and Lonsdale & Harmon (1991) have suggested, and Rowan-Robinson et al. (1993b) have confirmed, that the starburst galaxies detected by *IRAS*, which dominate the source counts at 60 μm, form the local counterpart to the faint submJy star-forming population (for comparison, the starburst galaxies in the QDOT sample were found to have a median redshift of 0.03).

Can the starburst component modelled in the IR provide the necessary contribution to the 1.4 GHz submJy radio source counts? The well-known correlation between the radio (interpreted as synchrotron emission from electrons leaking out of supernova remnants) and the FIR emission for spiral galaxies, $S(60\ \mu\mathrm{m}) = 90S(1.4\ \mathrm{GHz})$ (Helou et al. 1985; Condon, Anderson & Helou 1991b), is used to effect a shift in the 60-μm starburst luminosity function to 1.4 GHz. We use a power-law spectrum of $S_\nu \propto \nu^{-0.8}$ to obtain *K*-corrections, and pure luminosity evolution of the form used in the IR counts (equation 5). In Fig. 7, the normalized, differential source counts are plotted against observations [Windhorst, Dressler & Koo 1987; Mitchell & Condon 1985 (limits derived from fluctuation analysis)]. For the counts of the luminous radio sources (ellipticals), the model of Rowan-Robinson et al. (1993a) has been used, which provides a good fit to the data for fluxes greater than ≈ 1 mJy. The adopted model for the starburst galaxies fits the submJy data extremely well, confirming that we are indeed observing the same population of star-forming galaxies at both 60 μm and 1.4 GHz. Note that Hammer et al. (1995) have used the Canada France Redshift Survey (CFRS) to show that the optical counterparts to the fainter subμJy radio population consist of post-starburst galaxies, type 2 Seyfert AGN and early-type low-power AGN. Also shown in Fig. 7 is the non-evolving model which fails to fit the observed data. The form and rate of evolution used to fit the observed counts is very similar to that already used to represent quasars, as well as being identical to that in the IR, introducing the concept of a universal rate of evolution.

4 STARBURST GALAXY CONTRIBUTIONS TO SOURCE COUNTS IN THE NIR AND OPTICAL BANDS

4.1 Cosmological model

Having made detailed predictions for the source counts in the FIR we can now extend our models to investigate the contributions that the various IR populations make at other, shorter, wavelengths. Moving from the FIR to shorter wavelengths is, however, obviously more complex than just simply shifting the FIR luminosity function. Therefore, in this paper we will use a simple, standard model to represent the normal galaxies at shorter wavelengths and will focus our model predictions on the contribution of the starburst galaxy component to the *K*-, *I*- and *B*- photometric-band source counts.

We model the normal late-type galaxies (i.e. the extension of the IR cirrus component) in the NIR and optical bands with a model consisting of three galaxy types: Sab, Sbc and Sd/Im. The *K*-corrections from 1400–10 000 Å for these components are taken from the SEDs of Coleman, Wu & Weedman (1988), Yoshii & Takahara (1988) and Pence (1976), and a relative morphological mix of approximately equal proportion. In addition to the late-type normal galaxies, an elliptical component is introduced. E/S0 galaxies are expected to be much more prominent than they

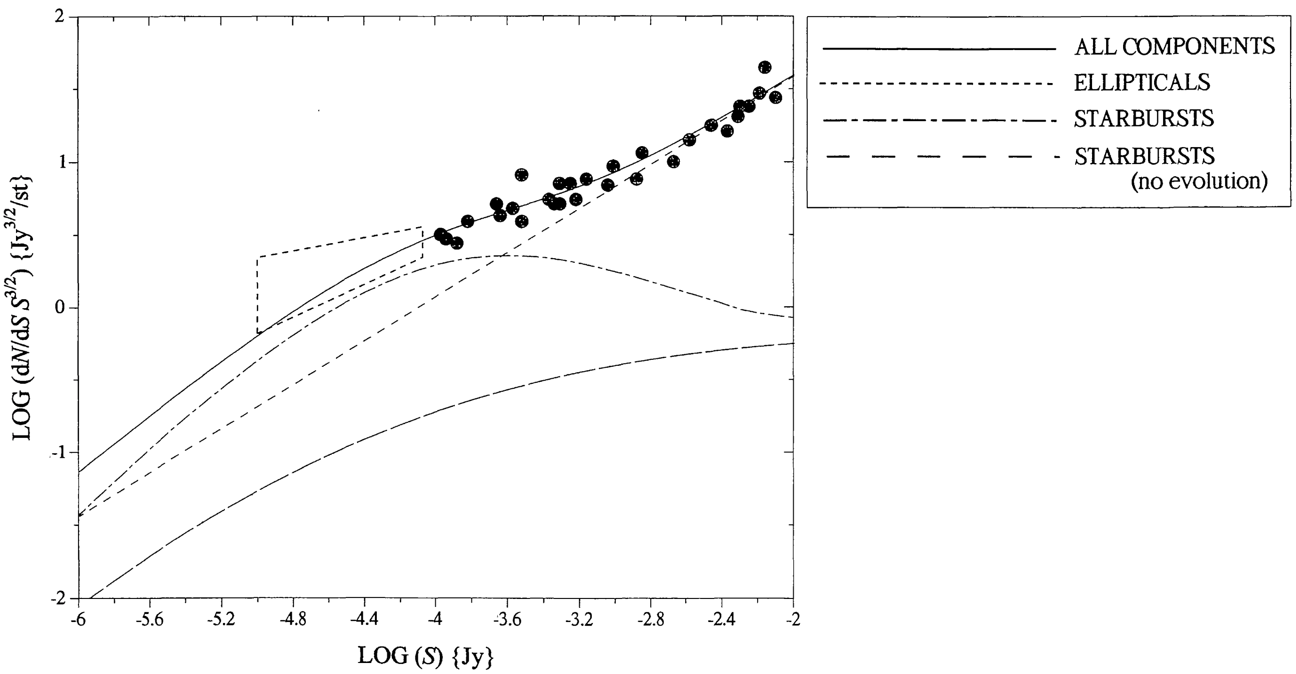

Figure 7. Fit of the starburst component, assuming pure luminosity evolution, to the observed submJy 1.4-GHz normalized differential counts described in the text. Also shown are the non-evolution case and the radio-loud elliptical component.

are at longer wavelengths because of the dominance of older stars. The K-corrections are derived from the spectral energy distributions of Yoshii & Takahara (1988) with the *IUE* data of Bertola, Capaccioli & Oke (1982) used for the UV with the relative local fractional mix of Shanks et al. (1984). In order to normalize the new optical/UV values with the original IR spectra, a re-radiation of $\approx$30 per cent of the optical light into the FIR is assumed for the late-type galaxies. This is in accordance with the work carried out by Rowan-Robinson et al. (1987) who found a mean value of $L_{60}/L_B=0.3$, and Corbelli, Salpeter & Dicky (1991) who found a mean value of 35 per cent.

The question of the suitable SED for the starburst galaxies is more complex. From 1 μm to the B band an Sab galaxy SED from Coleman et al. (1980) (see also Yoshii & Takahara 1988) has been chosen. McQuade, Calzetti & Kinney (1995), Storchi-Bergmann, Calzetti & Kinney (1994) and Kinney et al. (1993) have shown that star-forming galaxies cover a wide range of morphological types with flat or rising spectra from the blue band to the UV. To model the SED into the UV, several options were investigated including Im, H II, Sab and the blue star-forming galaxies NGC 4214 and 4670 observed by Huchra et al. (1983a). The best overall fit to the counts in the K, I and B bands is provided by using the SED of an Sab galaxy to just shortwards (in wavelength) of the B band and then using the spectrum of an H II galaxy at shorter wavelengths. The existence of galaxies with spectra almost identical to H II regions (see Shields 1990 for review) has been accepted for a long time (e.g. Zwicky 1966). Such galaxies are among the most luminous narrow-emission-line objects and possibly one of the youngest classes [due to a severe deficiency in heavy elements (see Terlevich 1987)] of galaxies observable. The power source behind such H II galaxies is thought to be an early, possibly primeval, population of O and B stars (e.g. French 1980). To model the H II component, the data for Mrk 36 compiled by Neugebauer et al. (1976) is used. They found that the spectrum is approximately constant or of very shallow gradient, consistent with the sample by Kinney et al. (1993) and models of starburst galaxies by Leitherer & Heckman (1995). To normalize the new spectrum to the original starburst spectrum, it is assumed that 5 per cent of the starlight leaks out at optical wavelengths with 95 per cent emerging in the IR, although some form of luminosity-dependent leakage (decreasing leakage with increasing luminosity) may mean that the brightest galaxies are not seen in B-band counts. This leakage is based upon the best fit to the B-band counts and is consistent with the strong IR excesses found for starburst galaxies by Leech et al. (1989).

The spectrum of the ultraluminous/hyperluminous component uses the SED of *IRAS* F10214, which has been analysed over the given wavelength range (see Rowan-Robinson et al. 1993a). In the case of this source, as little as 1 per cent of the optical light is likely to escape internal absorption by dust, making any detection in optical surveys unlikely.

In the NIR K and I bands, a Schecter luminosity function is used to represent the elliptical component (see below) but we maintain the use of the 60-μm luminosity function for the late-type galaxies so as to extend a connection between the FIR and NIR late-type galaxy populations. This has little effect on the overall counts.

To represent the luminosity function of normal galaxies in the optical we have chosen the type-dependent Schecter luminosity function of Loveday et al. (1992) [see Bingelli, Sandage & Tammann (1988) for review of the optical luminosity function]. This luminosity function was selected from the APM galaxy survey of Maddox et al. (1990a) and has been chosen because of the large volume of space covered and the lower bright-end normalization found as compared with other luminosity functions such as that of Efstathiou, Ellis & Peterson (1988), whose luminosity function is the average of five magnitude-limited redshift surveys (AARS:

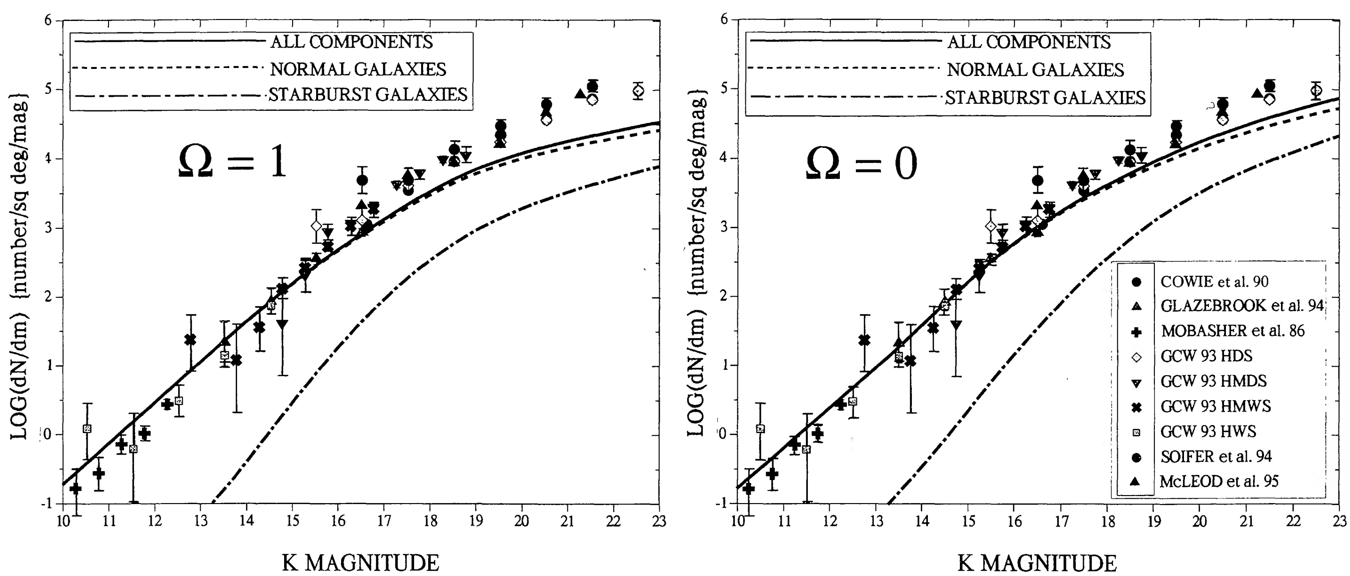

Figure 8. Model fits to the K-band observations described in the text, for closed and open geometries. The starburst galaxies have no effect on the global counts except at the faintest magnitudes.

Peterson et al. 1986; KOSS: Kirshner, Oemler & Schecter 1979; KOSS: Kirshner et al. 1983; RSA: Sandage & Tammann 1981; and CFA: Huchra et al. 1983b).

Following Schecter (1976), the Schecter function has the form

$$\varphi(M)\,\mathrm{d}M=\frac{2}{5}\ln(10)\,\phi^*\left(\frac{L}{L^*}\right)^{\alpha+1}\exp(-L/L^*)\,\mathrm{d}(M), \qquad (6)$$

$$L=10^{(M-4.75)/2.5}\,\mathrm{L}_\odot. \qquad (7)$$

Converting from magnitudes to luminosity, we have

$$\phi(L)=\frac{\mathrm{d}\Phi}{\mathrm{d}\log L}=\ln(10)\,\phi^*\left(\frac{L}{L^*}\right)^{\alpha+1}\exp(-L/L^*). \qquad (8)$$

The parameters for the model are given in Table 1.

For the starburst and hyperluminous galaxies we assume the luminosity function in both the NIR and optical bands is of the form in equation (4), shifted from 60-μm using the parameter $\Delta=L(\nu)/L_{60}$ as explained in Section 3.1.

The same form of pure luminosity evolution as was used in the FIR models is implemented for the starburst and hyperluminous components in the NIR and B band (see equation 5). Lonsdale & Chokshi (1993) have demonstrated that the blue and IR rates may be identical, although a steeper faint-end slope to the optical luminosity function may be required.

The normal galaxy components (spirals and ellipticals) are assumed to have no active evolution, but an element of passive evolution due to the natural aging of stars in the host galaxies is included. Although relatively complex models of stellar evolution such as those of Rocca-Volmerange & Guiderdoni (1988) and Bruzual & Charlot (1993) exist, because we are primarily interested in the starburst contribution we have simply used the population synthesis models of Arimoto & Yoshii (1986, 1987) and Yoshii & Takahara (1988), with the formulation of Mobasher, Sharples & Ellis (1993) to calculate the passive evolutionary correction. This is found by fitting a polynomial to the magnitude–redshift curve of each galaxy component.

4.2 Source counts in the NIR K and I bands

In the K band (2.2 μm) thermal re-radiation by dust, so dominant in the FIR, is replaced as the primary emission mechanism by radiation from the photospheres of long-lived stars. Thus evolution effects, due to, for example, enhanced star formation (involving the production of a population of young hot blue stars), are expected to be far less significant.

Fig. 8 shows the predicted K-band counts plotted in differential form per K magnitude using the magnitude/flux density conversion of Johnson (1966). A large number of extensive surveys in the K band (e.g. Mobasher, Sharples & Ellis 1986; Cowie et al. 1990; Glazebrook et al. 1994; Soifer et al. 1994; McLeod et al. 1995) have been carried out defining the source counts over a large range of magnitudes from $K=10$ to 30. Gardner, Cowie & Wainscoat (1993, hereafter GCW93) presented K-band source counts from four surveys [Hawaii Deep (HDS), Medium Deep (HMDS), Wide (HWS) and Medium Wide (HMWS) Surveys] and found that it was possible to fit the observations using two power laws with slopes of 0.67 for $10<K<16$ and 0.26 for $18<K<23$ with the turnover occurring somewhere between $K=16$ and 18. Our model reproduces broadly consistent slopes of 0.61 and 0.2 (for a closed universe) and 0.61 and 0.25 (for an open universe) respectively. The additional elliptical component accounts for approximately 50 per cent of the source counts for $K<20$, which is in agreement with the work of Franceschini et al. (1991). At fainter magnitudes, as expected, the spirals dominate the counts. Only at the faintest magnitudes (where the optical rest frame is sampled) does the evolving starburst component begin to affect the counts; at brighter K magnitudes the counts are well fitted by a non-evolving population as expected.

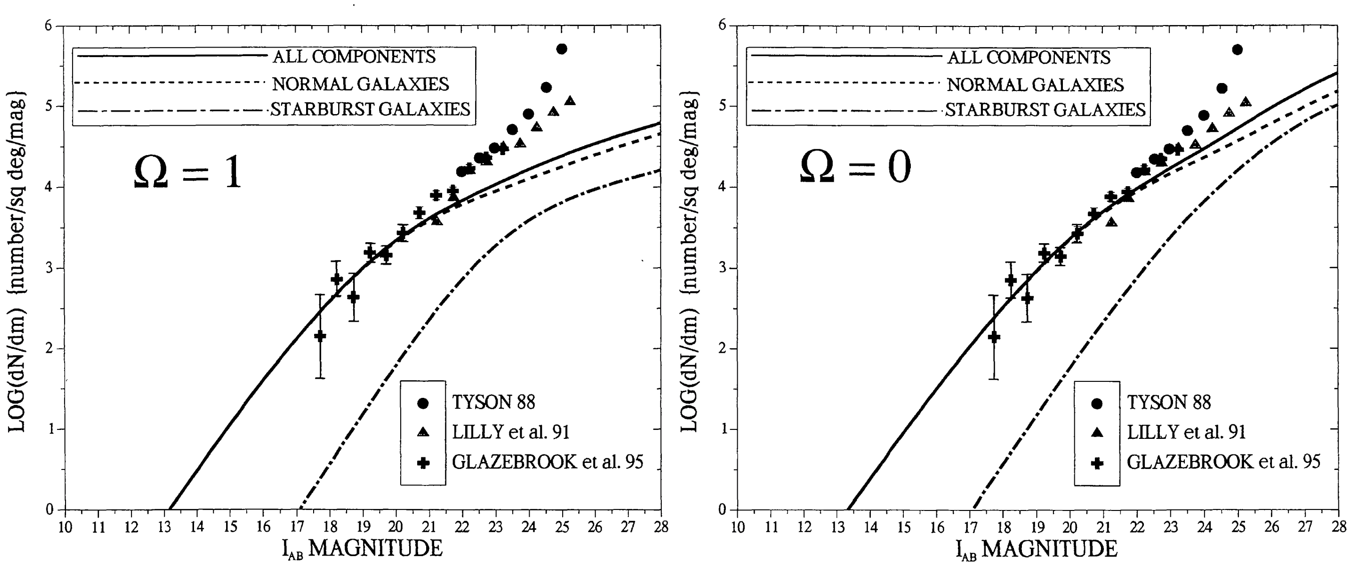

Figure 9. The fit of the model in a closed and an open universe to the I-band observations of Tyson (1988) and Lilly, Cowie & Gardner (1991). The model can only partially account for the faint excess.

Glazebrook et al. (1995a) find no evolution in the K band at $z<0.5$, consistent with a very low starburst contribution to the counts at the faintest magnitudes only. Not surprisingly, the hyperluminous component is negligible at these wavelengths and is not included in the figures. Here, as in the optical (although nothing like on the scale seen in the B band – see Section 6) we see an excess over the predictions. A lower value of the density parameter Ω_0 as suggested by Mobasher et al. (1993) significantly improves the fit to the observations, but Gardner et al. (1993) conclude that, at present, it is impossible to draw a clear conclusion on this (see Fig. 8b). Yobashii & Peterson have recently postulated that the K-band counts are fitted best by an open geometry and a non-zero cosmological constant. Changing the normalization of the starburst component, i.e. increasing the IR/optical leakage, will improve the fit to the faint end, although this normalization is constrained by the B-band counts to 5–10 per cent at the most.

Counts in the I band (≈ 0.9 μm) are much closer to the optical rest frame and hence are expected to produce a greater excess at fainter magnitudes than in the K band. Tyson (1988) and Lilly, Cowie & Gardner (1991) have recorded slopes of 0.34 and 0.32, respectively, although the errors at the faintest magnitudes are significant. Their counts were made in the I_{AB} band (AB magnitudes correspond to 3-arcsec apertures on the Canada-France-Hawaii Telescope), which can be roughly transformed to the standard values by $I_{AB} \sim I+0.48$. To constrain the model fully, reliable counts at brighter magnitudes are needed, and these have been taken from Glazebrook et al. (1995b). The model does not fare well in trying to reproduce these slopes, recording values of 0.19 and 0.26 for $\Omega=1$ and 0, respectively, from $22<I<26$. Once again the use of an open geometry improves the fit. The model fit to the observed source counts is shown in Fig. 9. Note that, although the total model slope is lower than observed, the starburst components have slopes of ~ 0.31 and 0.45 for $\Omega=1$ and, respectively, over the range $22<I<25$, much closer to the observed values. In both the K and I bands the optical rest frame is sampled at high redshift, thereby linking the NIR with the optical region. Any adopted SED for the starburst component will be simultaneously constrained by the counts in the K, I and B bands.

4.3 Starburst galaxy contributions in the optical *B* band

The optical B band is by far the most intensively studied wavelength in terms of source counts. In recent years, much work has been carried out producing source counts and redshift distributions in the optical (e.g. Tyson 1988; Lilly et al. 1991; Broadhurst, Ellis & Shanks 1988; Metcalfe et al. 1987). Results of these studies have shown that there exists a strong excess at faint magnitudes ($B>18$) over the predicted non-evolving results. The no-evolution models (e.g. Sandage 1988; Tyson 1988) predict a number–magnitude slope of $\mathrm{d}\log N(m)/\mathrm{d}m=0.6$ for bright magnitudes ($B<16$), flattening to about 0.4 at $B>19$, 0.3–0.36 at $B \approx 23$ and <0.2 at $B \approx 26$. In contrast, Broadhurst et al. (1988) find a slope of 0.4 at $20<B<23$ (compared with their no-evolution predictions of 0.32–0.34). Similarly, Tyson (1988) and Metcalfe et al. (1987) find slopes of 0.45 and 0.46 respectively in the range ($18<B<24$). From these results it is apparent that some form of evolution must be going on to produce the slope at the faint end of the counts. Galaxies were either more numerous or brighter in the past. However, redshift distributions from the Durham/AAT faint-galaxy redshift survey of over 200 galaxies (see Broadhurst et al. 1988) favour a non-evolving model. This paradox could be reconciled if evolution took place at the faint end of the luminosity function. Starburst in the recent past of such galaxies could then account for the blue excess.

Cowie, Songaila & Hu (1991) obtained K magnitudes and redshifts for a small (22) sample of galaxies down to $B=24$. They showed that the excess was caused by a large population of small blue galaxies between $z=0.2$ and 0.3. This raises the question of their whereabouts at the present epoch. Density-evolution models where these dwarf galaxies are treated as building blocks that have merged to create the galaxies we observe locally today are not well constrained, with a typical range of values of $(1+z)^{1.5-3.8}$ (e.g. Rocca-Volmerange & Guiderdoni 1990; Treyer & Silk 1993; Colin, Schramm & Peimbert 1994). Burkey et al. (1994) have used four deep fields observed with the *Hubble Space Telescope* to constrain the rate of merging between $z=0.7$ and the present epoch, and find that the merger range is fitted best by $(1+z)^{1.5\pm0.5}$, which corresponds to the disappearance, due to merging, of 13 per cent of the galaxy population. Density-evolution scenarios may face problems unless the merging galaxies were absorbed into larger galaxies [since independent merging within the population would result in elliptical galaxies that were too blue or spiral galaxies with discs that were too thick (Ostriker 1990)], or alternatively they could have just faded, implying a new population of objects containing a large amount of baryonic mass [but see McGaugh (1994) and Salzer (1994) for alternative explanations].

In this paper we assume that the excess is due to a new population of sources consisting either completely or partly of the *IRAS* starburst population seen at 60 μm. Lilly et al. (1991) and Broadhurst et al. (1988) both detected faint but very blue 'flat-spectrum' galaxies with strong [Ø II] line, with spectra identical to H II regions. The fraction of such galaxies was found to increase with redshift. Further evidence for star formation is provided by the *HST* observations of Griffiths et al. (1994) and Colless et al. (1994), who have shown that a large number of the faint blue galaxies (FBGs) have close companions and are interacting. Tresse et al. (1993) compiled a sample of the faint red, dwarf, sub-L^* ($<0.05L^*$) galaxies with $I>22.1$ and found that many showed signs of star formation. In the IR, Rowan-Robinson & Crawford (1989) showed that the IR colours for the *IRAS* starburst population were very similar to those of galactic H II regions. Could the *IRAS* starburst galaxies provide some fraction of the excess seen in the B band, at least to magnitudes of $B=20$–22 and possibly as faint as $B=22$–24 where the observations are a factor of 2 and 4–5 respectively above the non-evolution predictions (Maddox et al. 1990b)? Note that a new population of sources is not the sole remedy for the faint blue galaxy excess. A steeper than expected faint-end slope to the optical luminosity function is an alternative possibility (Lilly et al. 1995; Gronwall & Koo 1995; Colless 1995; Koo, Gronwall & Bruzual 1993; Eales 1993), although Glazebrook et al. (1995c) have used a recent redshift survey of 73 galaxies with median redshift of 0.46 to constrain any significant steepening of the local luminosity function faint-end slope.

The optical source counts are plotted in Fig. 10 in the B_J band. To convert between this band and that of Johnson (1966), the convention of Shanks et al. (1984) (see also Yoshii & Takahara 1988) where $B_J = B - 0.18$ has been used. Such a correction only affects the bright end of the counts, where the slope is steepest, and since this is only a relatively simple model any errors make such corrections insignificant.

From Fig. 10 it can be seen that the starburst galaxies begin to augment the source counts significantly at $B_J \sim 21$, where they comprise ≈ 18 per cent of the counts, and that they have a peak contribution at $B_J \approx 23$–24 in a closed universe where their contribution has risen to ~ 36 per cent. In an open universe the starburst contribution is approximately 50 per cent from $B_J \approx 24$ to the faintest magnitudes. Comparison of these fractions with observations are difficult due to the different selection criteria invoked to define the source population (i.e. starbursts) discussed here, but Broadhurst et al. (1988) found that the proportion of galaxies in the Durham/AAT survey with [O II] linewidths > 20 Å at $B_J \sim 21$ was ≈ 0.55. Koo & Kron (1992), however, report that about 20 per cent of galaxies at $B_J \sim 21$ have approximately flat spectra ($\alpha > -1$), rising to ~ 50 per cent by $B_J = 24$. At fainter magnitudes the starburst component cannot explain the observed excess although an open geometry provides a significantly better fit than the closed model.

Table 2 compares the slope (used here as an effective measure of the evolution) of the differential B-band counts of the model for closed and open universes, and also the isolated starburst component, with the corresponding observed values over three magnitude ranges. At bright magnitudes, both the model and the starburst component reproduce slopes close to the non-evolving value of 0.6. Moving to fainter magnitudes ($B_J = 20$–23), the slope of the model is preserved by the augmentation provided by the contribution from the starburst component. At the faintest magnitudes in a closed universe both the entire model and the starburst component

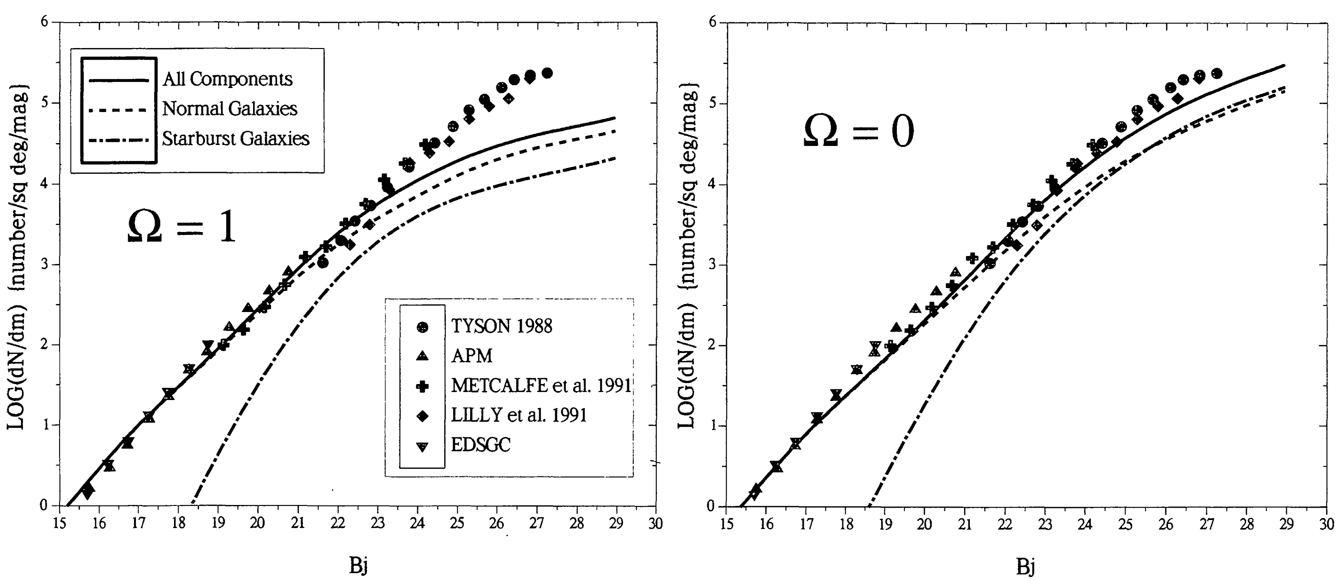

Figure 10. Comparison of the three-component model with the published B-band counts of Tyson (1988), Metcalfe et al. (1991), Lilly, Cowie & Gardner (1991), APM data and EDSGC data, compiled by Glazebrook et al. (1994). The normal galaxies are defined by a Schecter function with the parameters listed in Table 1. The starburst and hyperluminous components use the shifted 60-μm luminosity of Saunders. The addition of the starburst component can account for the excess to approximately $B_J = 20$–23 but still cannot explain the excess at fainter magnitudes. An open geometry provides a better fit to the observations than a closed universe.

Table 2. Comparison of B-band slope with observations and no-evolution predictions.

B_J -Magnitude	Model Total Ω=1	Model Total Ω=0	Model Starburst Ω=1	Model Starburst Ω=0	T88	S84	BES88	LCG91	No-evol.
<16	0.58	0.58	0.6	0.6					0.6
20-23	0.44	0.49	0.59	0.71		0.48	0.43		0.32-0.34
24-26	0.23	0.32	0.19	0.36	0.45			0.38	

Notes. T88: Tyson (1988); S84: Shanks et al. (1984); BES88: Broadhurst, Ellis & Shanks (1988); LCG91: Lilly, Cowie & Gardner (1991).

have slopes significantly lower than those observed, although when using an open geometry the discrepancies are not as severe.

These results are in agreement with Colless et al. (1993) and Broadhurst et al. (1988), who have suggested that starburst galaxies could be invoked to explain the excess in the range $B_J=20$–22 but that such models are in need of another population of sources to account for the counts at still fainter magnitudes. Tresse et al. (1996) have used the *I*-band Canada–France Redshift Survey to analyse a complete subsample of 139 field galaxies out to $z=0.3$. They suggest that the faint blue galaxy excess to $B=24$ cannot be due to star-forming galaxies because the ionization expected from the hot stars expected in a starburst galaxy cannot account for the observed line ratios. Instead, many of the galaxies in their sample have spectra indicative of type 2 Seyfert galaxies or LINERS. This result, however, appears to be at odds with most other spectroscopic studies of faint galaxies although a similar combination of AGN and starburst has been postulated for the faint 0.5–2 keV X-ray source counts from *ROSAT* (Pearson et al. 1996; McHardy et al., in preparation).

Owing to the luminosity evolution invoked to model the starburst galaxies, we predict that there exists a small high-redshift component to the counts at $B_J=20$–21 at $z\approx 2$ that was not observed by Broadhurst et al. (1988). Similar results have been obtained by Guiderdoni & Rocca-Volmerange (1990, 1991) and also more recently by Franceschini et al. (1994), who have modelled the optical counts using pure luminosity evolution. Their models find a substantial excess of galaxies at high redshift, although they reduce this by arguing that significant extinction by dust in the IR can reduce the observability of the galaxies in the optical. Campos & Shanks (1996) have emphasized the importance of dust extinction on the luminosity evolution of spiral galaxies at optical wavelengths. We have constrained this critical extinction fraction in starburst galaxies to approximately 95 per cent, consistent with the large IR excesses found by Leech et al. (1989). A value much lower than this will violate the observed counts at magnitudes of $B\approx 22$–24. The best option may be to incorporate both luminosity and density evolution into the models where the luminosity evolution is driven by mergers/interactions.

It is apparent that the number of starburst galaxies observed at these higher redshifts will depend critically on the amount of leakage assumed from the IR into the optical and the starburst SEDs. The SED needs to be strong enough in the optical to reconcile the counts at the faint end of the *K* and *I* bands but avoid producing a high-redshift component at medium *B* magnitudes and also have a UV component that can fit the faint *B*-band counts.

4.4 The IR/optical ratio in normal spiral galaxies

It is logical to assume that the normal galaxies seen in the optical can be associated with the cool cirrus galaxies seen at 60 μm in the IR, i.e. that the same population is being sampled in each waveband. In order to test this hypothesis, we implement a simple test where the traditional Schecter function used to represent the optical population of normal galaxies is used to represent the cirrus galaxies at 60 μm, which are presently well modelled by the Saunders lumino-

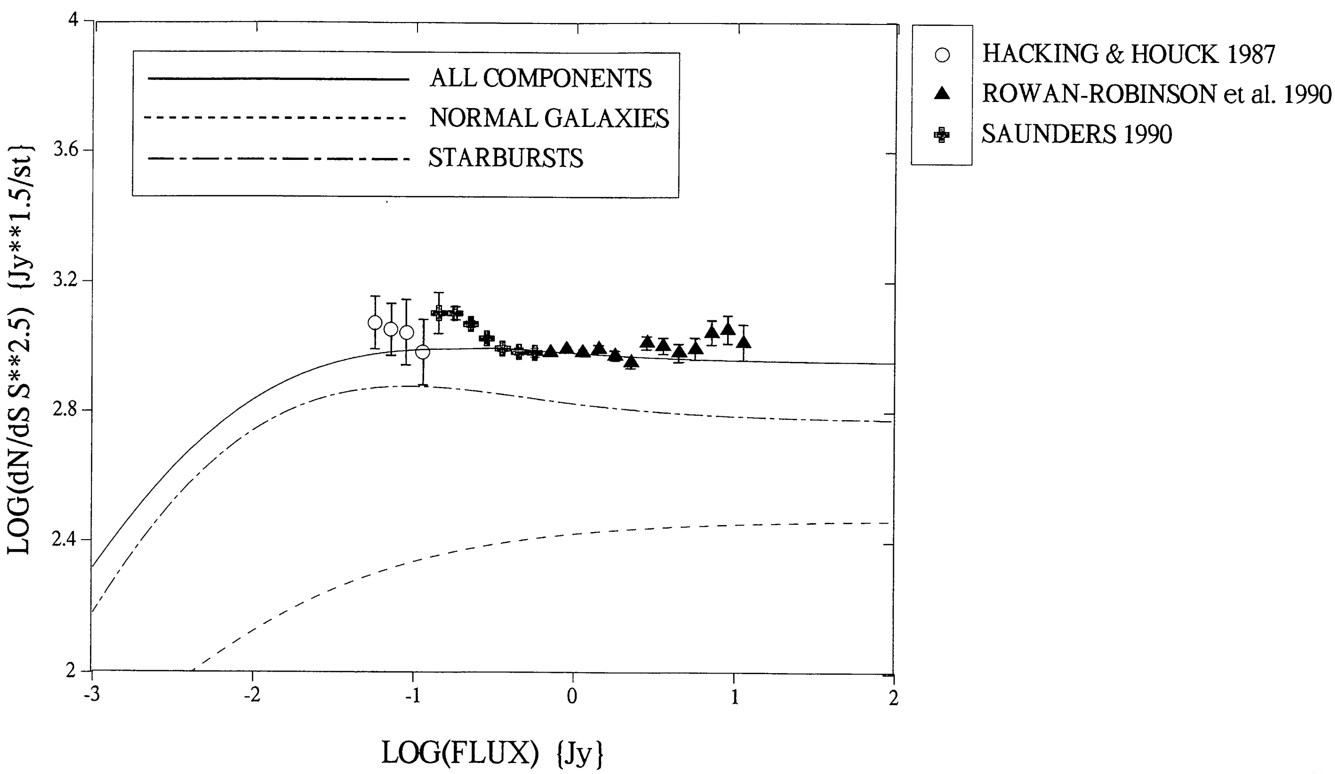

Figure 11. Fit to the observed counts at 60 μm using the shifted Schecter function to describe the cirrus galaxies assuming that we are seeing the same population of normal galaxies in both the *B* band and at 60 μm with 30 per cent of optical light re-radiated into the FIR.

sity function. The 60-μm luminosity function is broader than the optical Schecter function with a less steep decline with increasing luminosity, allowing more galaxies with luminosities greater than the characteristic luminosity L^* to be seen, so we do not expect a perfect fit to the 60-μm source counts.

The source counts at 60 μm have been reproduced using the Saunders luminosity function to model the starburst and hyperluminous galaxies and the Schecter function to model the cirrus component. The optical luminosity function is shifted to 60 μm using the same method as was used to model the source counts at wavelengths other than 60 μm with the Saunders function; i.e., the luminosity function is shifted by a factor L_B/L_{60}. We find that a ratio of ~ 30 per cent provides an adequate fit to the source counts. This simple model agrees well with the ratio of IR to optical light in galaxy samples studied by Rowan-Robinson et al. (1987) and Corbelli et al. (1991) and is indicative of a relatively low dust opacity in normal spiral galaxies. The fit to the 60-μm source counts is shown in Fig. 11 and is very good considering the simplicity of the assumptions applied.

Note that in moving from the optical to the IR there will also be a change in the galaxy morphological mix, introducing some uncertainty and margin for error into the results. In the optical, E/S0 galaxies account for about 20–28 per cent of the population (e.g. Kirshner, Oemler & Schecter 1978, 1979 and King & Ellis 1985), whereas they make an almost negligible contribution in the IR.

5 POSSIBLE FUTURE SURVEY STRATEGIES IN THE IR AND SUBMILLIMETRE

Using the predictions from the source counts in the IR and at submillimetre wavelengths, the predicted outcomes of possible forthcoming surveys using the next generation of satellites and ground-based observatories can be examined.

5.1 The *Infrared Space Observatory* (*ISO*)

The *Infrared Space Observatory*, launched in 1995 with a lifetime of 18 months, represents a major technological and scientific step forward over the earlier *IRAS* satellite. The 60-cm telescope has four main instruments: a camera (CAM), photometer (PHOT) and long- and short-wavelength spectrometers which will enable photometry, spectroscopy, imaging and polarimetry between 2.5 and 20 μm. The much increased sensitivity over *IRAS* (60 times deeper than the *IRAS* Point Source Catalogue at 60 μm and 2500 times deeper in the NIR) can be utilized to carry out extremely deep surveys over tens of degrees and would expect to discover thousands of normal, AGN and starburst galaxies, a significant fraction of which would be at high ($z > 1$) redshifts.

Several surveys are planned with *ISO* in both open and guaranteed time, mainly at wavelengths of 15 and 90 μm (Franceschini, Cesarsky & Roman-Robinson 1996). Such surveys are expected to be well matched to follow up ground-based observations at submillimetre mJy radio and optical wavelength. In addition, a slew survey at 200 μm is expected to cover a significant fraction of the sky to a sensitivity of the order of Jy. In Table 3 we present a summary of predicted source densities at these wavelengths from our IR model as a function of flux density. The actual numbers of sources detected and flux sensitivity in a given survey will of course depend critically on the survey area size.

In Figs 12 and 13 we present possible redshift distributions over an area of 25 square degrees at 90 and 15 μm respectively. At 90 μm the cirrus galaxies dominate at low redshift, with the starburst galaxies dominating at $z > 0.3$. The number of AGN predicted is of the order of tens, but with almost all (≥ 90 per cent) at high redshift. At 15μm the contribution from AGN is more significant, with approximately 25 per cent at $z > 1$, the proportion of type 1 and type 2 Seyferts being more or less equal at all fluxes. The results are consistent with those of Franceschini et al. (1992) who provide only lower limits for AGN.

The next possible successor missions to *ISO* are the Japanese *IRAS* mission due for lunch in 2001, NASA's *SIRTF* mission and ESA's *FIRST* mission. The *Far Infrared Space Telescope* (*FIRST*) is to be the fourth ESA Horizon 2000 cornerstone mission and is scheduled for launch in 2007. The 3.5-m telescope will have unprecedented sensitivity in the submillimetre region (for comparison, *IRAS* had a 60-cm mirror), being able to achieve a 5σ detection sensitivity of the order of 10 mJy in a 10-min integration time, at 200, 400 and 800 μm. An ultradeep survey of 10 square degrees taking up approximately 10 per cent of the observing time would be expected to discover over 6000 sources at 200 and 400 μm and about 800 at 800 μm, of which over 70 per cent would be expected to be starburst galaxies. Almost all (98 per cent) of the detected starburst galaxies at 800 μm would be at redshifts greater than 1.

5.2 The submillimetre common-user bolometer array

The Submillimetre Common User Bolometer Array (SCUBA), due for installation on the James Clerk Maxwell Telescope on Hawaii in 1996, promises to provide a signifi-

Table 3. Predicted source densities (per deg^2) at possible *ISO* survey wavelengths.

Sensitivity	200μm (Slew Survey) lg(number/sq. deg.)				90μm lg(number/sq. deg.)				15μm lg(number/sq. deg.)			
	Total	Normal	Starburst	AGN	Total	Normal	Starburst	AGN	Total	Normal	Starburst	AGN
1Jy	-0.13	-0.15	-1.55	-5.26	-0.22	-0.38	-0.77	-3.82	-2.09	-2.24	-2.85	-3.04
100mJy	1.55	1.35	1.13	-2.87	1.29	0.99	0.99	-1.69	-0.58	-0.75	-1.29	-1.49
10mJy	3.12	2.72	2.91	-0.67	2.69	2.16	2.54	0.50	0.92	0.71	0.29	0.14
1mJy	4.12	3.75	3.87	1.52	3.70	3.11	3.54	2.41	2.46	2.09	2.04	1.77
100μJy	4.74	4.42	4.43	3.19	4.42	3.89	4.16	3.58	3.72	3.32	3.31	3.06

cant increase in performance over the current UKT14 instrument (e.g. Gear 1994; Cunningham et al. 1994). Working at 850 and 450 μm with closely packed hexagonal arrays of 37 and 91 pixels, respectively, with a field of view of ≈0.0016 square degrees, SCUBA is expected to give a 10-fold increase in sensitivity, a 100-fold reduction in integration time and a 10 000-fold speed increase (at 450 μm) in survey speed over the current single detector. By using different filters it will also be possible to work at 750 and 350 μm with some loss of quality. Extra pixels are provided for 600 μm, 1.3 and 2 mm for broad-band photometry but no imaging capability.

It is apparent from the results of Section 3 that, because of the large *K*-corrections and evolution in the submilli-

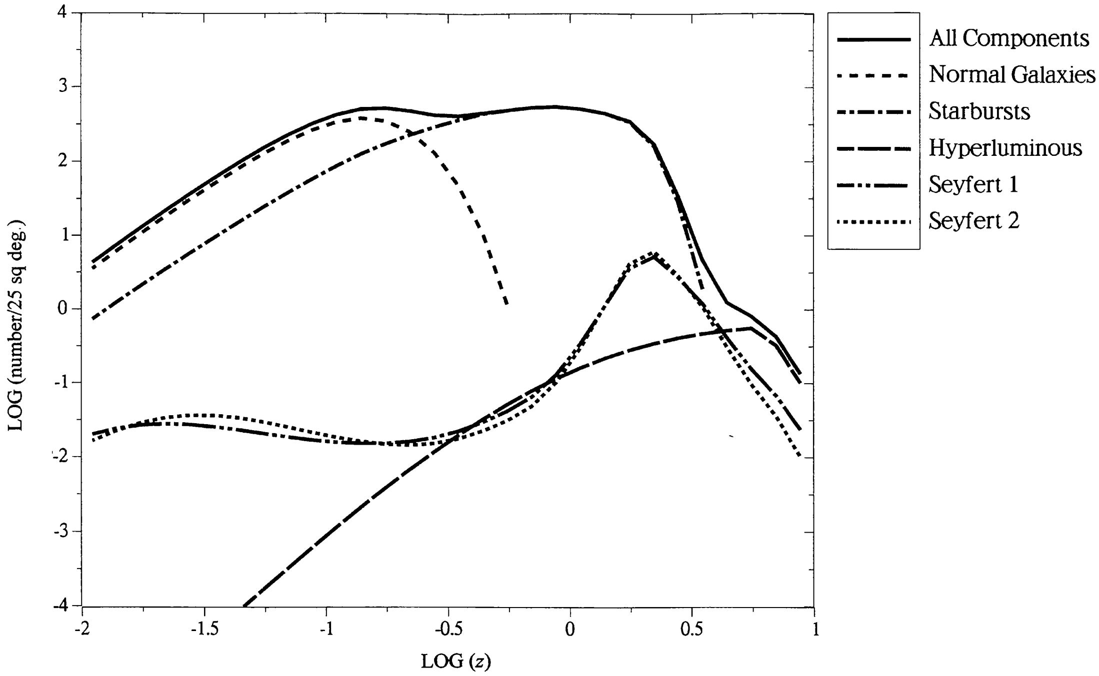

Figure 12. Predicted *N*–*z* distributions for the *ISO* ELAIS survey using the cirrus, starburst, hyperluminous and AGN components at 90 μm for a sensitivity of 15 mJy covering 25 deg^2.

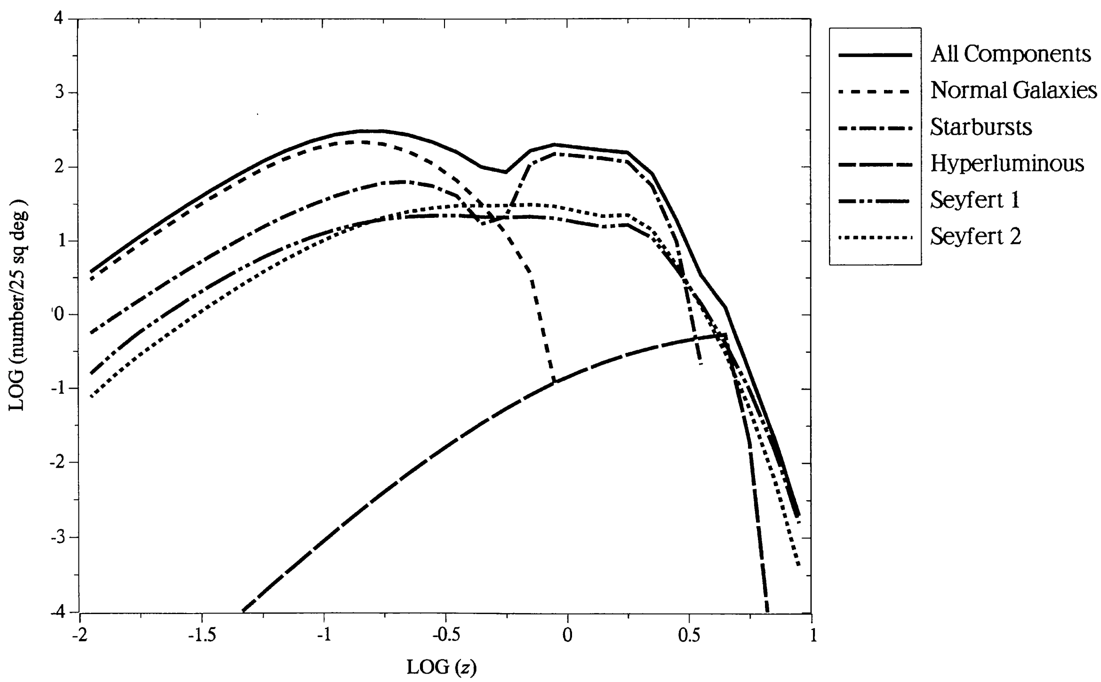

Figure 13. Predicted *N*–*z* distributions for the *ISO* ELAIS survey using the cirrus, starburst, hyperluminous and AGN components at 15 μm for a sensitivity of 1.7 mJy covering 25 deg^2.

Table 4. Statistics for a possible survey at 850 μm with SCUBA for 4.32×10^5 s observing time.

Survey Area (sq.deg.)	Integration time (s)	Limiting flux (5σ) {mJy}	Total number of sources detected	% of sources with z>1
691	1	300	18	3
1000	0.7	360	19	2
100	7	113	15	30
10	70	36	43	85
1	700	11	68	91

metre band, SCUBA will become a valuable tool for surveys for high-redshift galaxies (e.g. Blain & Longair 1996). We have used our models to predict the outcome of a variety of survey strategies based on a 10-d, 12-h or 20-d, 6-h (4.32×10^5 s) observing run (Rowan-Robinson et al., in preparation). The results are shown in Table 4. Expected sensitivities are at the moment extremely unsure, although, as a rough guide, on a good night one may expect an NEFD at 850 μm of $\approx$30 mJy $\mathrm{Hz}^{-1/2}$ (Griffin, private communication). To sample a given area on the sky completely, 16 telescope moves will be needed leading to an 8-fold increase (due to some data redundancy) in integration time. Surveys of areas of 1–10 square degrees are likely to lead to the detection of interesting numbers of sources, a high proportion of which will be expected to be $z > 1$.

A 1-square-degree ultra-deep survey at 850 μm would be expected to reveal approximately 70 high-redshift ($z > 1$) sources, which could possibly include more protogalaxy candidates such as F10214. Similar surveys at the other prime wavelength of 450 μm are not expected to be as successful, yielding only a dozen sources for a 1 deg^2 survey because the sensitivity at this shorter wavelength is poor compared to that at 850 μm.

6 CONCLUSIONS

We have presented a new model for cosmological source counts in the IR using the luminosity function for *IRAS* galaxies defined at 60 μm and a four-component model consisting of normal galaxies (cirrus), starburst galaxies, hyperluminous galaxies and AGN combined with pure luminosity evolution of the latter three components. The model provides an excellent fit to the observed normalized differential counts at 60 μm and confirms the large excess of sources expected in the FIR and submillimetre due to the shifting of the dust-emission hump through the observing band. The inversion of the flux–redshift relation, combined with the evolution, enhances the luminosity galaxies at high redshift, originally thought to have been out of our grasp, making them relatively easy to observe with the next generation of observatories (e.g. SCUBA, *IASO* and *FIRST*). Deep surveys from *ISO* and *FIRST* covering for example $\sim$20 square degrees would be expected to find thousands of sources, with a large proportion, between 30 and 98 per cent, of observed starburst galaxies in any sample having redshifts greater than 1. The 200-μm slew survey with *ISO* covering a large area of sky (thousands of square degrees) to 1 Jy will be well matched to searchers for hyperluminous galaxies, detecting of order 100. Ground-based observations with SCUBA favour a deep, small area survey, detecting $\approx$70 sources almost all at high redshift.

At other wavelengths, we have investigated the contribution to the source counts from starburst galaxies modelled by the warm *IRAS* population.

In the radio region at 1.4 GHz our model for the *IRAS* starburst population at 60 μm agrees with earlier conclusions that they are responsible for the submJy population that causes the upturn in the differential counts at faint fluxes. Strong luminosity evolution of the form $(1+z)^k$, $k=3.1$ is required. A lower value of $k=2$ is inadequate.

By introducing an elliptical component into our models we have extended our predictions to the NIR K and I bands, where we have shown that starburst galaxies are only expected to contribute at the very faintest magnitudes and that an open geometry is favoured over a closed universe for the form of evolution assumed here. However, no change in the cosmology can reconcile the models with the faint excess observed in the I band.

Using the observed counts in the optical B band as a constraint, the escape fraction of stellar light into the optical in starburst galaxies has been found to be between 5 and 10 per cent, with $\approx$95 per cent being re-radiated by dust in the FIR. Using the IR luminosity function, luminosity evolution, and treating the starburst galaxies in the optical as H II galaxies, we find that the starburst component can reconcile the faint blue galaxy excess to $B=20$–24, with the better fit being provided again by an open geometry. The addition of the starburst component cannot explain the excess at fainter magnitudes and a further population may be required. For normal spiral galaxies we show that IR cirrus sources are consistent with being associated with the optical spiral galaxies with an average of approximately 30 per cent re-radiation of the optical light into the IR, i.e. that spiral galaxies are optically thin.

REFERENCES

Arimoto N., Yoshii Y., 1986, A&A, 164, 260

Arimoto N., Yoshii Y., 1987, A&A, 173, 23

Beichman C. A., Helou G., 1991, ApJ, 370, L1

Benn C. R., Rowan-Robinson M., McMahon R. G., Broadhurst T. J., Lawrence A., 1993, MNRAS, 263, 98

Bertola F., Capaccioli M., Oke J. B., 1982, ApJ, 254, 494

Binggeli B., Sandage A., Tammann G. A., 1988, ARA&A, 26, 509

Blain A. W., Longair M. S., 1993, MNRAS, 264, 509

Blain A. W., Longair M. S., 1996, MNRAS, 279, 847
Boyle B. J., Fong R., Shanks T., Peterson B. A., 1987, MNRAS, 227, 717
Boyle B. J., Shanks T., Peterson B. A., 1988, MNRAS, 235, 935
Boyle B. J., Griffiths R. E., Shanks T., Stewart G. C., Georgantopoulos I., 1993, MNRAS, 260, 49
Broadhurst T. J., Ellis R. S., Shanks T., 1988, MNRAS, 235, 827
Bruzual G. A., Charlot S., 1993, ApJ, 405, 538
Burkey J. M., Keel W. C., Windhorst R. A., Franklin B. E., 1994, ApJ, 429, L13
Campos A., Shanks T., 1996, MNRAS, submitted
Chambers K. C., Charlot S., 1990, ApJ, 348, L1
Clements D. L. et al., 1996a, MNRAS, 279, 459
Clements D. L., Sutherland W. J., McMahon R. G., Saunders W., 1996b, MNRAS, 279, 477
Close L. M., Hall P. B., Liu C. T., Hege E. K., 1995, ApJ, 452, L9
Coleman G. D., Wu C., Weedman D. W., 1980, ApJS, 43, 393
Colin P., Schramm D. N., Peimbert M., 1994, APJ, 426, 459
Colless M., 1995, in Maddox S. J., Aragon A., eds, Wide-Field Spectroscopy and the Distant Universe. World Scientific, Singapore, p. 263
Colless M., Ellis R. S., Broadhurst T. J., Taylor K., Peterson B. A., 1993, MNRAS, 261, 19
Colless M., Scade D., Broadhurst T. J., Ellis R. S., 1994, MNRAS, 267, 1108
Condon J. J., 1984a, ApJ, 287, 5461
Condon J. J., 1984b, ApJ, 28, 44
Condon J. J., 1992, ARA&A, 30, 575
Condon J. J., O'Dell S. L., Puschell J. J., Stein W. A., 1981, ApJ, 246, 624
Condon J. J., Haung Z.-P., Yin Q. F., Thuan T. X., 1991a, ApJ, 378, 65
Condon J. J., Anderson M. L., Helou G., 1991b, ApJ, 376, 95
Corbelli E., Salpeter E., Dicky J. M., 1991, ApJ, 370, 49
Cowie L. L., Gardner J. P., Lilly S. J., McLean I. S., 1990, ApJ, 360, L1
Cowie L. L., Songaila A., Hu E. M., 1991, Nat, 354, 460
Cunningham C. R., Gear W. K., Duncan W. D., Hastings P. R., Holland W. S., 1994, Proc. SPIE Vol. 2198, Instrumentation in Astronomy VIII. p. 638
Danese L., De Zotti G., Franceschini A., Toffolatti L., 1987, ApJ, 318, L15
Della Ceca R., Maccacaro T., Gioia I. M., Stocke J. T., Wolter A., 1992, ApJ, 389, 491
Draine B. T., Lee H. M., 1984, ApJ, 285, 89
Dunlop J. S., Peacock J. A., 1990, MNRAS, 247, 19
Eales S., 1993, ApJ, 404, 51
Edelson R. A., Malkan M. A., Reike G. H., 1987, ApJ, 321, 233
Efstathiou G., Ellis R. S., Peterson B. A., 1988, MNRAS, 232, 431
Elbaz D., Arnaud M., Cassé M., Mirabel I. F., Prantzos N., Vangioni-Flam E., 1992, A&A, 265, L29
Elston R., McCarthy P. J., Eisenhardt P., Dickenson M., Spinrad H., Januzzi B. T., Mahoney P., 1994, AJ, 107, 910
Franceschini A., Danse L., De Zotti G., Xu C., 1988, MNRAS, 233, 175
Franceschini A., Toffolatti L., Mazzei P., Danese L., De Zotti G., 1991, A&S, 89, 285
Franceschini A., Mazzei P., De Zotti G., Danese L., 1994, ApJ, 427, 140
Franceschini A., Cesarsky C., Rowan-Robinson M., 1996, Memorie della Societa Astronomica Italiana, in press
French H. B., 1980, ApJ, 240, 41
Gardner J. P., Cowie L. L., Wainscoat R. J., 1993, ApJ, 415, L9 (GCW93)
Gautier T. N., Beichman C. A., 1985, BAAS, 16, 968
Gear W., 1994, The JCMT Newsletter, March, No. 2, 22
Glazebrook K., Peacock J. A., Collins C. A., Miller L., 1994, MNRAS, 266, 65
Glazebrook K., Peacock J. A., Miller L., Collins C. A., 1995a, MNRAS, 275, 169
Glazebrook K., Ellis R., Santiago B., Griffiths R., 1995b, MNRAS, 275, L19
Glazebrook K., Ellis R., Colless M., Broadhurst T., Allington-Smith J., Tanvir N., 1995c, MNRAS, 273, 157
Goldschmidt P., Miller L., La Franca F., Critiani S., 1992, MNRAS, 256, 65P
Graham J. R., Liu M. C., 1996, ApJL, submitted
Green S. M., Rowan-Robinson M., 1996, MNRAS, 279, 884
Griffiths R. E. et al., 1994, ApJ, 435, L19
Gronwall C., Koo D. C., 1995, ApJ, 440, L1
Guiderdoni B., Rocca-Volmerange B., 1990, A&A, 227, 362
Guiderdoni B., Rocca-Volmerange B., 1991, A&A, 252, 435
Hacking P. B., Houck J. R., 1987, ApJS, 63, 311
Hammer F., Crampton D., Lilly S. J., Le Fevre O., Kenet T., 1995, MNRAS, 276, 1085
Hauser M. G., 1995, COBE preprint 95-02, 1994, Proc. IAU Symp. 168, Examining the Big Bang and Diffuse Background Radiations. Kluwer, Dordrecht, in press
Helou G., Soifer B. T., Rowan-Robinson M., 1985, ApJ, 298, L7
Hildebrand R. H., 1983, QJRAS, 24, 267
Huchra J. F., Geller M. J., Gallagher J., Hunter D., Hartmann L., Fabbiano G., Aaronson M., 1983a, ApJ, 274, 125
Huchra J. P., Davis M., Latham D., Tonry J., 1983b, ApJS, 52, 89
Hughes D. H., Robson E. I., Dunlop J. S., Gear W. K., 1993, MNRAS, 263, 607
Johnson H. L., 1966, ARA&A, 4, 193
King C. R., Ellis R. S., 1985, ApJ, 288, 456
Kinney A. L., Bohlin R. C., Calzetti D., Panagia N., Wyse R. F. G., 1993, Ap&SS, 86, 5
Kirshner R. P., Oemler A., Schecter P. L., 1978, AJ, 83, 1549
Kirshner R. P., Oemler A., Schecter P. L., 1979, AJ, 84, 951
Kirshner R. P., Oemler A., Schecter P. L., Schectman S. A., 1993, ApJ, 88, 1285
Koo D. C., Kron R. G., 1992, AR&A, 30, 613
Koo D. C., Gromwall C., Buzual G. A., 1993, ApJ, 415, L21
Lawrence A., Walker D., Rowan-Robinson M., Leech K. J., Penston M. V., 1986, MNRAS, 219, 687
Lawrence A. et al., 1993, MNRAS, 260, 28
Lawrence A., Rigopoulou D., Rowan-Robinson M., McMahon R. G., Broadhurst T., Lonsdale C. J., 1994, MNRAS, 266, L41
Leech K. J., Penston M. V., Terlevich R., Lawrence A., Rowan-Robinson M., Crawford J., 1989, MNRAS, 240, 349
Leitherer C., Heckman T. M., 1995, Ap&SS, 96, 9
Lilly S. J., Cowie L. L., Gardner J. P., 1991, ApJ, 369, 79
Lilly S. J., Le Fevre O., Hammer F., Crampton D., Tresse L., 1995, in Maddox S. J., Aragon A., eds, Wide-Field Spectroscopy and the Distant Universe. World Scientific, Singapore, p. 281
Lonsdale C. J., Chokshi A., 1993, AJ, 105, 1333
Lonsdale C. J., Harmon R. T., 1991, Adv. Space Res., 11, 255
Lonsdale C. J., Hacking P. B., Conrow T. P., Rowan-Robinson M., 1990, ApJ, 358, 60
Lonsdale C. J., Smith H. E., Lonsdale C. J., 1995, ApJ, 438, 632
Loveday J., Peterson B. A., Efstathiou G., Maddox S. J., 1992, 390, 338
Low F. J. et al., 1984, ApJ, 278, L19
Maccacaro T., Della Ceca R., Gioia I. M., Morris S. L., Stocke J. T., Wolter A., 1991, ApJ, 374, 117
McGaugh S. S., 1994, Nat, 367, 538
McLeod B. A., Bernstein G. M., Rieke M. J., Tollestrup E. V., Fazio G. G., 1995, ApJS, 96, 117
McQuade K., Calzetti D., Kinney A. L., 1995, ApJS, 97, 331
Maddox S. J., Sutherland W. J., Efstathiou G., Loveday J., 1990a, MNRAS, 243, 692

Maddox S. J., Sutherland W. J., Efstathiou G., Loveday J., Peterson B. A., 1990b, MNRAS, 247, 1P
Mather J. C. et al., 1994, ApJ, 420, 439
Mathis J. S., 1990, ARA&A, 28, 37
Matthews et al., 1994, ApJ, 420, L13
Metcalfe N., Fong R., Jones L. R., Shanks T., 1987, in Bergeron J., Kunth D., Rocca-Volmerange B., Tran Thanh Van J., eds, High Redshift, Primeval Galaxies. Editions Frontières, Gif-sur-Yvette, p. 37
Metcalfe N., Shanks T., Fong R., Jones L. R., 1991, MNRAS, 249, 498
Miller L., Goldschmidt P., La Franca F., Cristiani S., 1993, in Chincarini G., Iovino A., Maccacaro T., Maccagni D., eds, ASP Conf. Ser. 51, Observational Cosmology. Astron. Soc. Pac., San Francisco, p. 614
Mitchell K. J., Condon J. J., 1985, ApJ, 90, 1957
Mobasher B., Sharples R. M., Ellis R. S., 1986, MNRAS, 223, 11
Mobasher B., Sharples R. M., Ellis R. S., 1993, MNRAS, 263, 560
Moshir M. et al., 1989, The Explanatory Supplement to the IRAS Faint Source Survey. JPL, Pasadena
Narlikar J. V., 1993, Introduction to Cosmology. Cambridge Univ. Press, Cambridge
Neugebauer G., Becklin E. E., Oke J. B., Searle L., 1976, ApJ, 205, 29
Norman C., Scoville N., 1988, ApJ, 332, 124
Oliver S. J., Rowan-Robinson M., Saunders W., 1992, MNRAS, 256, 15P
Oliver S. J. et al., 1995, in Maddox S. J., Aragon A., eds, Wide-Field Spectroscopy and the Distant Universe. World Scientific, Singapore, p. 274
Ostriker J. P., 1990, in Kron R. G., ed., The Evolution of the Universe of Galaxies. Astron. Soc. Pac., San Francisco, p. 25
Padovani P., 1993, MNRAS, 263, 461
Pearson C. P., Rowan-Robinson M., McHardy I. M., Jones L. R., Mason K. O., 1996, MNRAS, submitted
Pence W., 1976, ApJ, 203, 39
Peterson B. A., Ellis R. S., Efstathiou G., Shanks T., Bean A. J., Fong R., Zen-Long Z., 1986, MNRAS, 221, 233
Rigopoulou D., Lawrence A., Rowan-Robinson M., 1996, MNRAS, 278, 1069
Rocca-Volmerange B., Guiderdoni B., 1988, A&AS, 75, 93
Rocca-Volmerange B., Guiderdoni B., 1990, MNRAS, 247, 166
Rowan-Robinson M., 1970, MNRAS, 149, 365
Rowan-Robinson M., 1980, ApJS, 44, 403
Rowan-Robinson M., 1986, MNRAS, 219, 737
Rowan-Robinson M., 1991, Adv. Space Res., 11, 247
Rowan-Robinson M., 1992, MNRAS, 258, 787
Rowan-Robinson M., 1995, MNRAS, 272, 737
Rowan-Robinson M., Crawford J., 1989, MNRAS, 238, 523
Rowan-Robinson M., Efstathiou A., 1993, MNRAS, 263, 675
Rowan-Robinson M., Hughes J., Vedi K., Walker D. W., 1990, MNRAS, 246, 273
Rowan-Robinson M. et al., 1991, Nat, 351, 719
Rowan-Robinson M., Efstathiou A., Lawrence A., Oliver S., Taylor A., 1993a, MNRAS, 261, 513
Rowan-Robinson M., Benn C. R., Lawrence A., McMahon R. G., Broadhurst T. J., 1993b, MNRAS, 263, 123
Rush B., Malkan M. A., Spinoglio L., 1993, ApJS, 89, 1
Salzer J. J., 1994, Nat, 367, 510
Sandage A., 1988, ARA&A, 26, 561
Sandage A., Tammann G. A., 1981, A Revised Shapley–Ames Catalog of Bright Galaxies. Carnegie Institution of Washington, Washington
Saunders W., 1990, PhD thesis, Queen Mary, Westfield College, Univ. London
Saunders W., Rowan-Robinson M., Lawrence A., Efstathiou G., Kaiser N., Ellis R. S., Frenk C. S., 1990, MNRAS, 242, 318
Savage B. D., Mathis J. S., 1979, ARA&A, 17, 73
Schecter P., 1976, ApJ, 203, 297
Shanks T., Steveson P. R. F., Fong R., MacGillivray H. T., 1984, MNRAS, 206, 767
Shields G. A., 1990, ARA&A, 28, 525
Soifer B. T., Houck J. R., Neugebauer G., 1987, ARA&A, 25, 187
Soifer B. T. et al., 1994, ApJ, 420, L1
Solomon P. M., Downes D., Radford S. J. E., 1992, ApJ, 398, L29
Sopp H., Alexander P., 1991, MNRAS, 251, 112
Sopp H., Alexander P., 1992, MNRAS, 259, 425
Storchi-Bergmann T., Calzetti D., Kinney A. L., 1994, ApJ, 429, 572
Telesco C. M., 1993, MNRAS, 263, L37
Terlevich R., 1987, in Bergeron J., Kunth D., Rocca-Volmerange B., Tran Thanh Van J., eds, High Redshift, Primeval Galaxies. Editions Frontières, Gif-sur-Yvette, p. 281
Terlevich R., Melnick J., 1985, MNRAS, 213, 841
Thuan T. X., Condon J. J., 1987, ApJ, 322, L9
Trentham N., 1995, MNRAS, 277, 616
Tresse L., Hammer F., le Fèvre O., Proust D., 1993, A&A, 277, 53
Tresse L., Rola C., Hammer F., Stasinska G., 1996, in Maddox S., Aragon-Salamanca A., eds, Proc. 35th Herstmonceux Conf., Wide Field Spectroscopy and the Distant Universe. World Scientific, Singapore, in press
Treyer M.-A., Silk J., 1993, ApJ, 408, L1
Tyson J. A., 1988, ApJ, 96, 1
Vaceli M. S., Viegas S. M., Gruenwald R., Benevides-Soares P., 1993, Instituto Astronomico e Geofisico, preprint no. 038
Weedman D. W., Fieldman F. R., Balanzo V. A., Ramsey L. W., Sramek R. A., Wu C. C., 1981, ApJ, 248, 105
Windhorst R. A., 1984, PhD thesis, Univ. Leiden
Windhorst R. A., Dressler A., Koo D. C., 1987, in Hewit A., Burbidge G., Fang L. Z., eds, Observational Cosmology. Reidel, Dordrecht, p. 573
Yoshii Y., Peterson B. A., 1995, ApJ, 444, 15
Yoshii Y., Takahara F., 1988, ApJ, 326, 1
Zwicky F., 1966, ApJ, 143, 192